



Contents lists available at ScienceDirect

## Perspectives in Plant Ecology, Evolution and Systematics

journal homepage: [www.elsevier.com/locate/ppees](http://www.elsevier.com/locate/ppees)

## Research article

Phylogeny of Sesuvioideae (Aizoaceae) – Biogeography, leaf anatomy and the evolution of C<sub>4</sub> photosynthesisKatharina Bohley<sup>a,1</sup>, Olga Joos<sup>a,1</sup>, Heidrun Hartmann<sup>b</sup>, Rowan Sage<sup>d</sup>, Sigrid Liede-Schumann<sup>c</sup>, Gudrun Kadereit<sup>a,\*</sup><sup>a</sup> Institut für Allgemeine und Spezielle Botanik und Botanischer Garten der Johannes Gutenberg-Universität Mainz, D-55099 Mainz, Germany<sup>b</sup> Biozentrum Klein Flottbeck, Ohnhorststr. 18, DE-22609 Hamburg, Germany<sup>c</sup> Department of Plant Systematics, University of Bayreuth, DE-95517 Bayreuth, Germany<sup>d</sup> Department of Ecology and Evolutionary Biology, University of Toronto, 25 Willcocks Street, Toronto, ON M5S3B2 Canada

## ARTICLE INFO

## Article history:

Received 18 July 2014

Received in revised form

24 November 2014

Accepted 18 December 2014

Available online xxx

## Keywords:

Carbon isotope values

Character evolution

Kranz anatomy

*Sesuvium**Trianthema*

Water storage tissue

## ABSTRACT

Sesuvioideae (Aizoaceae) form a small subfamily of drought-tolerant plants exhibiting leaf succulence, halophytic ecology, and the C<sub>4</sub> photosynthetic pathway. Sesuvioideae are sister to the species-rich subfamilies Ruschioideae, Mesembryanthemoideae and Aizooideae that contain many CAM lineages. This close relationship of CAM and C<sub>4</sub> taxa identifies the Sesuvioideae as an important clade to address hypotheses of photosynthetic pathway evolution. This study presents a molecular phylogeny of Sesuvioideae based on five markers (*atpB-rbcL* spacer, *rps16* intron, *trnL-trnF* spacer, *petB-petD* spacer, ITS) and 51 accessions representing all genera and 37 species. We determined carbon isotope data of 103 samples and examined the leaf anatomy of 25 species. A RASP (Reconstruct Ancestral State in Phylogenies) analysis was used to reconstruct the ancestral biogeography of Sesuvioideae and trace its current worldwide distribution. Maximum likelihood character optimization was conducted for six traits related to photosynthetic type and leaf anatomy to characterize the evolution of leaf types in Sesuvioideae. The well-resolved molecular phylogeny revealed an African/Arabian origin of the subfamily with *Tribulocarpus* as sister to a clade containing *Trianthema*, *Sesuvium*, *Cypselea* and *Zaleya*. Intercontinental dispersal occurred within *Trianthema* (to Australia and South America) and *Sesuvium/Zaleya* (to Australia and North/Central America). Character optimizations favoured a single origin of C<sub>4</sub> photosynthesis with two reversions to the C<sub>3</sub> state, one within American *Sesuvium* and the other in *Trianthema* subgenus *Trianthema*. However, biochemical diversity of the C<sub>4</sub> syndrome in Sesuvioideae might indicate multiple origins of the C<sub>4</sub> pathway. Two C<sub>3</sub> and four C<sub>4</sub> anatomical types (atriplicoid, salsoloid, portulaceloid and pilosoid) are present in the subfamily, based on differences in water storage tissue, vascular bundle arrangements, and chlorenchyma structure. Ancestral state reconstruction indicates multiple losses or reduction of water storage tissue in the subfamily and frequent shifts in leaf anatomical traits.

© 2015 Geobotanisches Institut ETH, Stiftung Ruebel. Published by Elsevier GmbH. All rights reserved.

## Introduction

Sesuvioideae is the smallest subfamily of Aizoaceae, containing some 60 species of annual and perennial, often prostrate herbs and some woody shrubs (Fig. 1; Hartmann, 2001a, 2001b). The subfamily occurs mainly in subtropical regions of Australia and Africa with some species scattered in Asia and the Americas. One of the most common is the widespread coastal species *Sesuvium*

*portulacastrum* L., which occurs in disturbed estuaries and shorelines protected from surf, most often in mangroves. Many members of the subfamily grow on saline soils or in disturbed semi-arid habitats of lower latitude, typically in hot climates (Fig. 1; Hartmann, 2001a, 2001b). Morphological and molecular phylogenetic studies demonstrate that Sesuvioideae is sister to all other subfamilies of Aizoaceae (Ruschioideae, Mesembryanthemoideae and Aizooideae; Bittrich and Hartmann, 1988; Klak et al., 2003; Thiede, 2004) containing five genera, *Cypselea* Turp., *Sesuvium* L., *Trianthema* L., *Tribulocarpus* S. Moore and *Zaleya* Burm.f. (Fig. 1; Hassan et al., 2005; Thulin et al., 2012). The split between Sesuvioideae and its sister clade dates back to the early Miocene (Forest and Chase, 2009; Klak et al., 2004; Wikström et al., 2001 for

\* Corresponding author. Tel.: +49 61313922537.

E-mail address: [clausing@uni-mainz.de](mailto:clausing@uni-mainz.de) (G. Kadereit).<sup>1</sup> These authors contributed equally to this paper.



**Fig. 1.** Members of Sesuvioideae. (A) and (B) *Trianthema parvifolia*, South Namibia, near Aussenkehr, desert, in shallow depressions along the road (photos D. U. Bellstedt). (C) *T. sheilae* (photo H. Hartmann), (D) *T. crystallina* (photo H. Hartmann), (E) *Trianthema vleiensis* (photo H. Hartmann), (F) *Cypselea humifusa* on the muddy lakebed of the Spangler Springs Reservoir, near Lahonton, Nevada, USA, (G) and (H) *Sesuvium verrucosum*, USA, Nevada, Lahonton Reservoir lakebed (photos R. Sage).

age of Aizoaceae). The sister clades, particularly the Ruschioideae, extensively diversified during the late Miocene and produced approximately 1770 extant species (Valente et al., 2013), while the Sesuvioideae remained species-poor (Klak et al., 2004).

The Aizoaceae is one of the few angiosperm families with both, C<sub>4</sub> and CAM photosynthetic pathways, in addition to C<sub>3</sub>. Other families with both pathways are Euphorbiaceae, Asteraceae and Portulacaceae (Sage, 2002). In Aizoaceae, C<sub>4</sub> photosynthesis is only known to occur within the Sesuvioideae and has not been detected in the sister subfamilies Ruschioideae, Mesembryanthemoideae and Aizooideae. By contrast, CAM is unknown in Sesuvioideae but common in the other three subfamilies. Information on the distribution of photosynthetic pathways is incomplete in the Sesuvioideae, however, such that the relative numbers of C<sub>3</sub> and C<sub>4</sub> species are unclear and the possibility of CAM Sesuvioideae species

cannot be ruled out. Succulence is common to all of the subfamilies of the Aizoaceae. Ruschioideae, Mesembryanthemoideae and Aizooideae differ from Sesuvioideae by an endoscopic orientation of the peripheral vascular bundles (Melo-de-Pinna et al., 2014).

Within the Sesuvioideae, C<sub>4</sub> photosynthesis is known for nine species: *Trianthema compacta* T.C. White, *Trianthema pilosa* F. Muell., *Trianthema portulacastrum* L., *Trianthema sheilae* A.G. Mill. & J.A. Nyberg, *Trianthema sedifolia* Vis., *Trianthema triquetra* Willd., *Cypselea humifusa* Turpin, *Zaleya pentandra* (L.) Jeffr., *Zaleya galericulata* (Melville) H. Eichler, *Z. decandra* (L.) Burm.f. and *Sesuvium sesuvoides* Verdc. (Bittrich, 1990; Carolin et al., 1978; Downton, 1975; Muhibit et al., 2007; Muhibit and McKown, 2013; Raghavendra and Das, 1978). Both major biochemical subtypes of C<sub>4</sub> photosynthesis normally found in the eudicots, NADP-malic enzyme (NADP-ME) and NAD-ME, are present in Sesuvioideae

(Muhaidat et al., 2007). Interestingly, there is high activity of PEP-CK (a further decarboxylating enzyme which is more common in monocots) in NADP-ME *T. portulacastrum* and NAD-ME *Z. pentandra* (Muhaidat and McKown, 2013). The only anatomical type documented in the Sesuvioidae is the atriplicoid-type, but only a few species have been studied (Carolin et al., 1978; Muhaidat et al., 2007). Multiple C<sub>4</sub> anatomical types have been identified in numerous families of hot, arid and/or saline habitats, most notable in the Chenopodiaceae (Jacobs, 2001; Freitag and Kadereit, 2013; Kadereit et al., 2003; Schütze et al., 2003) and Portulacaceae (Voznesenskaya et al., 2010) in which succulence is common in sister lineages to C<sub>4</sub> clades (Kadereit et al., 2012; Ocampo et al., 2013). Together, these observations indicate that the Sesuvioidae may be a hotspot for C<sub>4</sub> evolution, potentially evolving multiple lineages with diverse types of C<sub>4</sub> metabolism and anatomy.

The significance of succulence for photosynthetic evolution has been discussed over the years, but remains suggestive. Succulence in C<sub>3</sub> taxa is proposed to be an important enabler of CAM evolution because it provides a convenient storage site for nocturnal acid accumulation based on PEP carboxylation of respiratory CO<sub>2</sub>, as may occur in proto-CAM ancestors (Ogburn and Edwards, 2013; Sage, 2002). However, no Chenopodiaceae taxa are known to be CAM, and the succulence in these plants may be associated with salt accumulation as part of the halophytic life form (Flowers and Colmer, 2008). Weak CAM activity is evident in the Portulacaceae, most of whose species are succulent C<sub>4</sub> species (Ocampo et al., 2013). Succulence may constrain the evolution of typical forms of kranz anatomy, where mesophyll (M) cells are present in single radial layers around inflated bundle sheath (BS) cells that in turn surround leaf veins (Dengler and Nelson, 1999). Most eudicots exhibit this typical kranz anatomy, as exemplified by the Atriploid type (Edwards and Voznesenskaya, 2011; Sage et al., 2011). In C<sub>4</sub> leaves, it is essential that the M cells lie close to the BS tissue in order to minimize diffusion distances between cells (Bräutigam and Weber, 2011), and pre-existing succulence may interfere with close arrangements of M and typical BS cells, thus necessitating alternative versions of kranz anatomy should it be possible to evolve C<sub>4</sub> (Kadereit et al., 2014). Consistently, the Chenopodiaceae and Portulacaceae exhibit the greatest diversity in C<sub>4</sub> structural types in the eudicots (Edwards and Voznesenskaya, 2011; Freitag and Kadereit, 2013; Kadereit et al., 2003; Ocampo et al., 2013). To fully evaluate the hypothesis that succulence promotes diversity of C<sub>4</sub> anatomies, additional, unrelated lineages of C<sub>4</sub> evolution should be examined. Given the similarities in ecology and life form to the Chenopodiaceae and Portulacaceae, yet their distant relationship within Caryophyllales (Christin et al., 2011), the Sesuvioidae is a strong candidate to further evaluate evolutionary relationships between succulence and the potential diversification of C<sub>4</sub> leaf anatomy.

At present, our current knowledge of when and where C<sub>4</sub> photosynthesis evolved in the Sesuvioidae is incomplete, owing to incomplete species coverage in previous molecular analyses (Hassan et al., 2005; Thulin et al., 2012) as well as limited analysis of leaf anatomy and photosynthetic pathway distributions within the subfamily. To establish the Sesuvioidae as a model for studying C<sub>4</sub> plant evolution, it is necessary to produce a detailed molecular phylogeny including most species of the subfamily and then map photosynthetic pathway and anatomical characteristics onto this phylogeny. Here, we present a comprehensive and well-resolved molecular phylogeny based on five markers (*atpB-rbcL* intergenic spacer, *rps16* gene intron, *trnL-trnF* intergenic spacer, *petB-petD* intergenic spacer and ITS), a leaf anatomical survey, a survey of carbon isotope ratios ( $\delta^{13}\text{C}$ ), and a biogeographic analysis of the origin of Sesuvioidae. This combination of measurements provides the first detailed account of C<sub>4</sub> evolution and leaf anatomical diversity in the Sesuvioidae.

## Materials and methods

### Plant material and sampling

Herbarium samples were largely used for the molecular and anatomical studies although we included a few plants grown in the greenhouse at the Mainz Botanical Garden from seeds or cuttings collected in the wild. Table 1 lists the species analyzed while online supplemental Table 1 presents voucher information for all accessions.

### Sequencing and phylogenetic inference

Fifty-one accessions were included in the phylogenetic analyses representing all genera of Sesuvioidae, *Tribulocarpus* (both spp.), *Trianthema* (22 spp. representing both subgenera), *Zaleya* (3 spp.), *Sesuvium* (9 spp.) and *Cypselea* (1 sp.). Five additional accessions were included representing the other subfamilies of the Aizoaceae (*Gibbaeum pachypodium* L. Bolus, *Aptenia cordifolia* (L.f.) Schwantes, *Cryophyllum crystallinum* (L.) N.E. Br., *Tetragonia tetragonoides* (Pall.) Kuntze, *Delosperma cooperi* L. Bolus). Furthermore, *Phytolacca dioica* L. (Phytolaccaceae) was used as an outgroup according to the results of Christin et al. (2011) and Bissinger et al. (2014). Table 1 presents sequences generated for this study and downloaded accessions from GenBank ([www.ncbi.nlm.nih.gov/genbank/](http://www.ncbi.nlm.nih.gov/genbank/)).

Total DNA was extracted from dried or fresh leaf material using the DNeasy Plant Mini Kit (QIAGEN, Germany) following the manufacturer's protocol. PCRs for five markers (*atpB-rbcL* intergenic spacer, *rps16* gene intron, *trnL-trnF* intergenic spacer, *petB-petD* intergenic spacer, ITS) were carried out in T-Professional or T-Gradient Thermocycler (Biometra, Germany) or PTC100 Thermocycler (MJ Research, USA) using the primers, PCR recipes and cycler programmes listed in Table 2. PCR-products were checked on 0.8% agarose gels and purified using the NucleoSpin® Gel and PCR clean-up-Kit (Macherey-Nagel, Germany) following the manufacturers manual. The Big Dye® Terminator v3.1 Cycle Sequencing Kit (Applied Biosystems) combined with the primers mentioned above were used for the sequencing reaction followed by a purification step using IllustraTM SephadexTM G-50 Fine DNA Grade (GE Healthcare, UK). Sequencing was performed following the Sanger method on a 3130xl Genetic Analyzer (Applied Biosystems Inc., USA). The raw forward and reverse sequences were checked and combined in Sequencher 4.1.4 (Gene Codes Corporation, USA). The alignment was done by hand in Seaview 4 (Gouy et al., 2010) and Mesquite 2.75 (Maddison and Maddison, 2011). The programme sequence matrix (v. 1.7.8; Vaidya et al., 2011) was used to combine the five matrices.

Maximum Likelihood analyses for (1) the combined cp data, (2) ITS and (3) all markers combined were performed using RAxML version 7.7.1 (Stamatakis, 2006; Stamatakis et al., 2008) using GTR+G as substitution model. *P. dioica* was defined as outgroup.

Additionally, trees were generated using BEAST v1.5.4 (Bayesian Evolutionary Analysis by Sampling Trees; Drummond and Rambaut, 2007; Rambaut and Drummond, 2003) for the combined matrix. The BEAST xml input files were generated with BEAUTi v1.5.4 (Drummond and Rambaut, 2007). Monophyly of the ingroup (all Aizoaceae) was constrained in order to root the tree with one outgroup taxon, *P. dioica*. The following settings were chosen: substitution model parameters GTR+G with four categories for G, relaxed clock model with exponential distribution and a birth and death demographic model (Drummond et al., 2006). The MCMC was initiated two times independently on a random starting tree with 20,000,000 iterations and sampling frequency of 1000. Convergence of model parameters was confirmed using TRACER

**Table 1**

Taxa of Sesuvioideae and outgroups included in molecular analyses, anatomical and isotopic studies. For the molecular markers and isotopic values the number of accessions studied is indicated. Further details and voucher information can be found in Tables 3 and 4, as well as in the supplemental Tables 1 and 2.

Taxon	ITS	rps16	trnL-F	atpB-rbcL	Anatomical sections	Isotope values
<i>Phytolacca dioica</i> L. (Phytolaccaceae) – outgroup	JX232571	AJ532733	AJ558037	AJ532612	–	–
<i>Tetragonia tetragonoides</i> (Pall.) Kuntze	1	1	1	1	–	–
<i>Aptenia cordifolia</i> (L. f.) Schwantes	1	1	1	1	–	–
<i>Cryophyllum crystallinum</i> (L.) N.E. Br. (= <i>Mesembryanthemum crystallinum</i> L.)	1	1	1	1	Kondo et al. (1998)	–
<i>Gibbaeum pachypodium</i> L. Bolus	1	1	1	1	+	–
<i>Delosperma cooperi</i> L. Bolus	1	1	1	1	Konrad et al. (2013)	–
<i>Cypselea humifusa</i> Turpin	1	1	1	1	Muhaidat et al. (2007)	4
<i>Sesuvium congense</i> Welw. ex Oliver	1	1	1	1	+	1
<i>Sesuvium crithmoides</i> Welw.	1	1	1	1	+	2
<i>Sesuvium marinum</i> (Walter) Stern, Britton & Poggenb.	2	2	2	2	+	3
<i>Sesuvium portulacastrum</i> L.	9	7	9	7	+	7
<i>Sesuvium sessile</i> Pers.	1	1	1	0	–	3
<i>Sesuvium sesuvioides</i> (Fenzl) Verdc. <sup>a</sup>	5	5	4	5	+	13
<i>Sesuvium verrucosum</i> Raf.	3	3	3	3	+	8
<i>Trianthema argentina</i> Hunz. & Cocucci	1	1	1	1	–	1
<i>Trianthema ceratosepala</i> Volkens & Irmsch.	1	–	1	–	+	3
<i>Trianthema clavata</i> (J.M. Black) H.E.K. Hartmann & Liede	1	1	1	1	–	–
<i>Trianthema compacta</i> C.T. White	AJ937565	1	–	–	–	1
<i>Trianthema corallicola</i> H.E.K. Hartmann & Liede	–	1	1	1	+	1
<i>Trianthema corymbosa</i> (Sonner) H.E.K. Hartmann & Liede	1	1	1	1	+	2
<i>Trianthema crystallina</i> A.G. Mill. & J.A. Nyberg	1	1	1	1	+	1
<i>Trianthema megasperma</i> A.M. Prescott	1	1	1	1	–	–
<i>Trianthema oxyacalypta</i> F. Muell.	1	1	1	–	–	3
<i>Trianthema parvifolia</i> E. Meyer ex Sonder	AJ577769	HE585069	HE585094	–	+	2
<i>Trianthema patellifecta</i> A.M. Prescott	1	1	1	1	–	–
<i>Trianthema pilosa</i> F. Muell.	1	1	1	1	+	2
<i>Trianthema portulacastrum</i> L.	1	1	1	1	Muhaidat et al. (2007), Muhaidat and McKown (2013)	4
<i>Trianthema rhynchocalyptra</i> F. Muell.	1	1	1	1	–	2
<i>Trianthema salsolooides</i> Fenzl ex Oliv.	1	1	1	1	+	3
<i>Trianthema sedifolia</i> Vis.	1 + HE585052	1 + HE585075	1 + HE585097	1	+	5
<i>Trianthema sheliae</i> A.G. Mill. & J.A. Nyberg	HE585053	HE585076	HE585098	–	+	–
<i>Trianthema transvaalensis</i> Schinz	–	1	1	–	+	–
<i>Trianthema turgidifolia</i> F. Muell.	AJ937580	HE585077	–	–	–	1
<i>Trianthema ufoensis</i> H.E.K. Hartmann & Liede	HE585054	HE585078	HE585099	–	–	–
<i>Trianthema vleiensis</i> H.E.K. Hartmann & Liede	1	1	1	1	+	–
<i>Tribulocarpus dimorphanthus</i> S. Moore	1	1	1	1	+	1
<i>Tribulocarpus retusus</i> (Thulin) Thulin & Liede	1	1	1	1	+	–
<i>Zaleya galericulata</i> (Melville) H. Eichler	1	1	1	1	Carolin et al. (1978)	3
<i>Zaleya pentandra</i> (L.) C. Jeffrey	1	1	1	1	+	6
<i>Zaleya redimita</i> (Melville) Bhandari	1	1	1	1	–	1

<sup>a</sup> Including *S. hydaspicum* (Edgew.) Gonç. and *S. nyasicum* (Baker) Gonç. Our data do not support the separation of these species from *S. sesuvioides* as suggested by Gonçalves (1965), but further investigations are needed to resolve the *S. sesuvioides* species complex.

(Rambaut and Drummond, 2003). Burn-in values were determined empirically from the likelihood values and PP clade support was calculated together with the medians and 95% confidence limits for ages of the nodes. The post-burn in tree sample was sub-sampled to obtain c. 1000 trees for use in the biogeographical analysis and for character optimization of the photosynthetic type. For ancestral character reconstruction of anatomical traits a second BEAST analysis was conducted excluding all species for which no anatomical data could be obtained (missing data entries in Table 3). The remaining data set comprised 25 species of Sesuvioideae and *C. crystallinum* as outgroup. The analysis was conducted as described above.

#### Biogeographical analysis with RASP (reconstruct ancestral state in phylogenies)

The biogeographical analysis was done with RASP v. 2.1b (Yu et al., 2013) using 1000 randomly sampled trees generated with BEAST (see previous paragraph). To prevent forcing into a narrow, potentially incorrect area, we assumed a widely distributed ancestor in reconstructing the ancestral distribution. The species distribution was coded with A=Africa and Saudi Arabia,

B=Australia, C=North and Central America, D=South America and E=Asia (Table 3). For all species except *Sesuvium portulacastrum* L., the entire distribution area of the species was coded for the terminals included in the tree. In case of the multiple accessions of the widespread *S. portulacastrum*, the actual origin of the sample was coded. *Phytolacca dioica* was defined as the outgroup and a majority rule consensus tree was generated. Afterwards a Bayesian Binary MCMC analysis with standard “Gamma” variation was conducted and a maximum distribution of four regions per node from each of the five coded areas allowed. All other settings were in the default mode.

#### $\delta^{13}\text{C}$ isotopic analysis and leaf anatomy

Carbon isotope ratios relative to the Pee Dee belemnite standard were measured on 103 samples of dried leaf material representing 44 species in order to determine the photosynthetic pathway (online supplemental Table 2). Samples were analyzed by the University of California, Davis isotope facility (<http://stableisotopefacility.ucdavis.edu>) or the Institut für Geowissenschaften at the Johannes Gutenberg-Universität, Mainz.

**Table 2**

Primers, PCR recipes and cycler programme.

Marker	Primer sequences and references	PCR recipe ( $\mu$ l)	Cycler programme
ITS	P17S 5'-CAT CCG ATT GAA TGG TCC GGT GAA-3' P26S 5'-TCC CCG TTC GCT CGC CGT TAC TA-3' (both Popp and Oxelman, 2001)	ddH <sub>2</sub> O 16.55, MgCl <sub>2</sub> (50 mg/ml) 2, buffer 2.5, dNTPs (10 $\mu$ M) 0.25, taq polymerase 0.2, F primer (10 $\mu$ M) 1, R primer (10 $\mu$ M) 1, DNA template 1.5	97 °C for 90 s, 35 cycles of [97 °C for 20 s, 69 °C for 90 s, 72 °C for 90 s], 72 °C for 7 min
<i>petB-petD</i>	pipetB1411F 5'-GCC GTM TTT ATG TTA ATG C-3' pipetD738R 5'-AAT TTA GCY CTT AAT ACA GG-3' (both Schäferhoff et al., 2009)	ddH <sub>2</sub> O 16.5, MgCl <sub>2</sub> (50 mg/ml) 1, buffer 2.5, dNTPs (10 $\mu$ M) 0.5, taq polymerase 0.5, F primer (10 $\mu$ M) 1, R primer (10 $\mu$ M) 1, DNA template 2	96 °C for 90 s, 35 cycles of [95 °C for 30 s, 52 °C for 1 min, 72 °C for 90 s], 72 °C for 20 min
<i>rps16-intron</i>	<i>rps16</i> F 5'-GTC GTA GAA AGC AAC GTG CGA CTT-3' (Oxelman et al., 1997); <i>rps16internR</i> 5'-CTT GTT CCG GAA TCC TTT ATC-3'; <i>rps16internF</i> 5'-GTA TGT TGC TGC CAT TTT TGA AAG G-3'; <i>rps16</i> R2 5'-TCG GGA TCG AAC ATC AAT TGC AAC-3' (Oxelman et al. 1997)	ddH <sub>2</sub> O 17.54, MgCl <sub>2</sub> (50 mg/ml) 1.5, buffer 3.68, BSA 0.03, dNTPs (10 $\mu$ M) 0.5, taq polymerase 0.25, F primer (10 $\mu$ M) 0.25, R primer (10 $\mu$ M) 0.25, DNA template 1	80 °C for 5 min, 35 cycles of [95 °C for 1 min, 50 °C-65 °C* for 1 min, 65 °C for 4 min], 65 °C for 5 min *increasing in 0.3 °C steps
<i>atpB-rbcL</i> spacer	<i>atpB-rbcL</i> -spacer F 5'-GAA GTA GAA TTG ATT CTC-3'; <i>atpB-rbcL</i> -spacer R 5'-CAA CAC TTG CCT TAG TCT CTG-3' (both Golenberg et al., 1993)	ddH <sub>2</sub> O 19.25, MgCl <sub>2</sub> (50 mg/ml) 1, buffer 2.5, BSA 0.25, dNTPs (10 $\mu$ M) 0.25, taq-polymerase 0.25, F primer (10 $\mu$ M) 0.5, R primer (10 $\mu$ M) 0.5, DNA template 0.5	94 °C for 1 min, 35 cycles of [94 °C for 20 s, 56 °C for 30 s, 72 °C for 60 s], 94 °C for 20 s, 56 °C for 80 s, 72 °C for 8 min
<i>trnL-F</i>	Tab C 5'-CGA AAT CGG TAG ACG CTA CG-3'; Tab D 5'-GGG GAT AGA CGG ACT TGA AC-3' (both Taberlet et al., 1991); <i>trnL-F</i> internF 5'-GGA CGA GAA TGA AGA TAG ACT C-3'; TabF 5'ATI' TGA ACT GGT GAC ACG AG 3' (Taberlet et al., 1991)		

Sectioning herbarium material of succulent plants is problematic and the quality of the resulting sections largely depends on the success of the first step in which the material is soaked for 7–10 days in 10%-ammonia solution. Slow dehydration with an ascending ethanol series and embedding either in paraffin or Technovit 7100 (Heraeus-Kulzer, Germany) followed the soaking. We used three different staining methods, (1) toluidine blue solution, (2) W-3A-staining following the protocol of Wacker (2006) or (3) a special mixture of Azur II (Merck AG, Germany), Eosin Y (Merck AG, Germany), and methylene blue (Merck AG, Germany). For a detailed protocol of sample preparation for sectioning and staining of slides see online supplemental material.

#### Ancestral character state reconstruction

Photosynthetic type (trait 1) and six leaf anatomical traits (traits 2–6) were coded in a multistate matrix (Table 3). C<sub>3</sub> and CAM were summarized as one photosynthetic character state assuming that C<sub>3</sub> would be the ancestral condition in the Ruschioideae/Mesembryanthemoideae/Aizoideae clade. The photosynthetic type was coded according to carbon isotope measurements given in Table 4 with C<sub>3</sub> and CAM = 0 and C<sub>4</sub> = 1. Leaf anatomical traits were coded as follows: trait 2 “water storage tissue (WST)”: no or little WST = 0, distinct WST = 1; trait 3 “hypodermis”: not present = 0, present = 1 (a hypodermis was only coded as present when a layer of non-photosynthetic, hypodermal cells surrounded the entire leaf); trait 4 “position of kranz layer”: 0 = absent, 1 = kranz layer around individual vascular bundles, 2 = continuous, peripheral kranz layer; trait 5 “shape of cross section”: flat = 0, round/rounded = 1; trait 6 “bladder cells”: 0 = epidermis cells large or small, but not bulging, 1 = large, bulging epidermis cells present. In order to infer ancestral states for each of the traits described above, individual optimisations were performed on the binary characters under ML in Mesquite V.2.7 (Maddison and Maddison, 2011) over 1000 post-burn-in trees from the BEAST analysis summarized on the MCC tree. Under ML, the fit of single (One-parameter Markov-k-state model) versus 2-rate models (asymmetrical 2-parameter Markov k-state model) as implemented in Mesquite given the MCC tree was tested using a likelihood ratio test. For trait 4 “position of kranz layer” as a

multistate character only the application of the One-parameter Markov-k-state model was possible.

#### Results

##### Phylogenetic inference

Maximum likelihood trees resulting from cpDNA data and ITS alone did not exhibit conflicting topologies. Topological differences never received bootstrap support > 50. Therefore, a combined matrix was used for further analyses. This matrix comprised 57 accessions and 4799 aligned positions of which 2234 were variable. The ML tree search resulted in a well-resolved phylogram (Fig. 2) which did not conflict with the topology found in the Bayesian analysis (not shown). Sesuvioideae are monophyletic (bootstrap (BS) 100). *Tribulocarpus* is sister to the remaining genera (BS 100). *Trianthema* is monophyletic (BS 86) and sister to a *Zaleya/Sesuvium/Cypselea* (BS 84) clade. The two subgenera of *Trianthema* are monophyletic (*T. subgenus Papularia* BS 100 and *T. subgenus Trianthema* BS 100). *Zaleya* is monophyletic (BS 100) and sister to a paraphyletic *Sesuvium* including *Cypselea* (BS 100). Infra-generic and infrageneric relationships are partially resolved in *Trianthema* and *Sesuvium* (Fig. 2).

##### Biogeographical analysis

Our reconstruction of the geographic distribution shows that Africa and Saudi Arabia are the most likely ancestral regions for Sesuvioideae (Fig. 2). Dispersal from this area to North and Central America occurred in the common ancestor of the *Sesuvium/Cypselea* lineage and subsequently this lineage seems to have repeatedly reached South America in several widespread species. Dispersal from Africa/Arabia to Australia occurred three times: once within *Zaleya* (*Z. galericulata*), a second time within *Trianthema* subgenus *Trianthema* and the third time within *Trianthema* subgenus *Papularia* (*Trianthema ufoensis* H.E.K. Hartmann & Liede and *Trianthema clavata* (J.M. Black) H.E.K. Hartmann & Liede; Fig. 2). The latter lineage also shows a dispersal event from Africa to South America. East Asian regions were only reached by the globally distributed *S. portulacastrum* and *T. portulacastrum*.

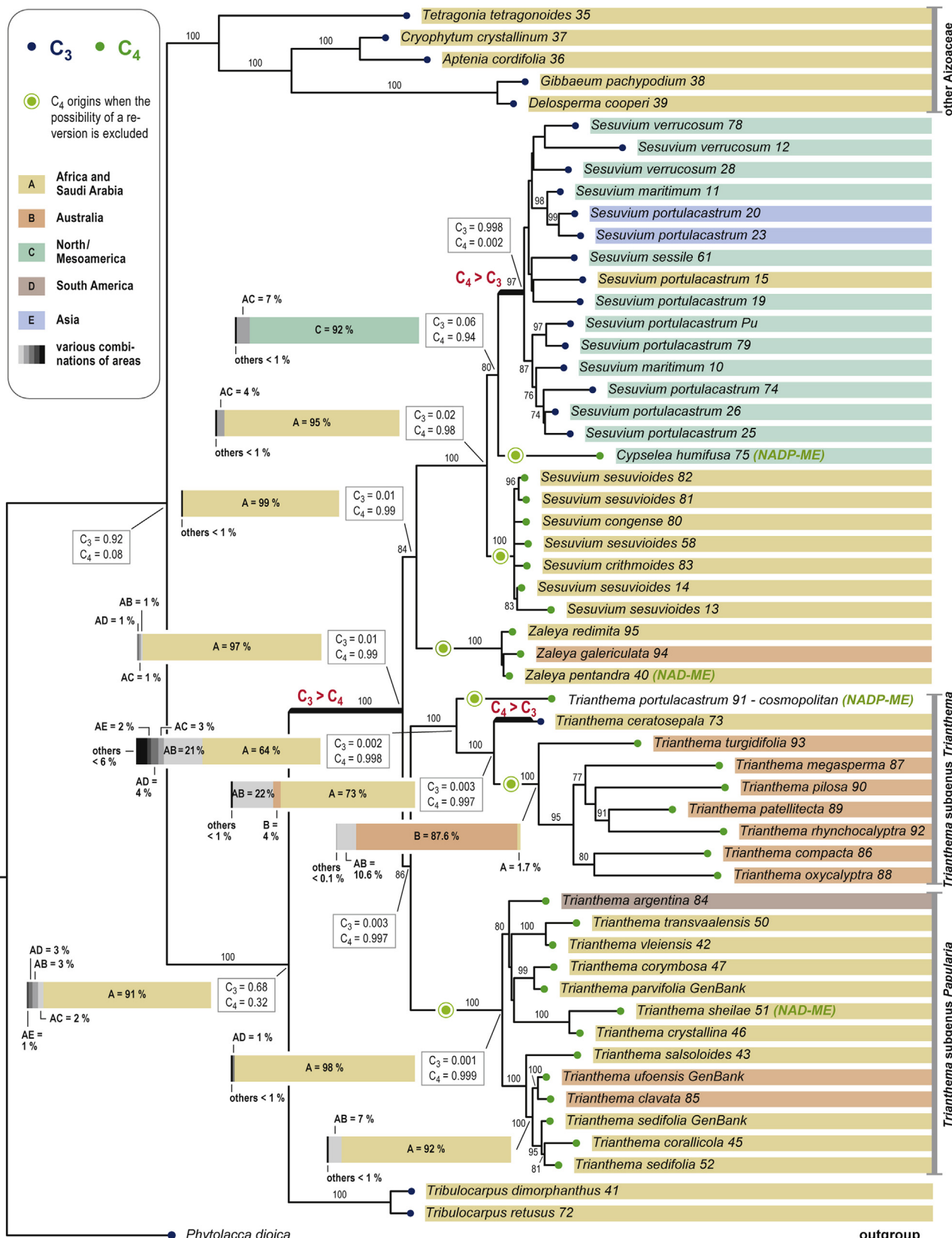


**Fig. 2.** Molecular phylogeny of Sesuvioideae based on the combined analysis of five markers (*atpB-rbcL* intergenic spacer, *rps16* gene intron, *trnL-trnF* intergenic spacer, *petB-petD* intergenic spacer, ITS), 51 accessions representing 37 species and all genera of the subfamily and maximum likelihood inference. The photosynthetic pathway ( $C_3$  or  $C_4$ ) is traced over the tree using ML optimization and proportional likelihoods for character states at selected nodes are indicated (white boxes). An alternative scenario of  $C_4$  evolution excluding the possibility of a reversion is indicated by green dots showing the multiple origins of  $C_4$  photosynthesis. The results of a biogeographical analysis are indicated by horizontal bars which illustrate the frequency of reconstructed ancestral areas over 1000 random trees resulting from a Bayesian analysis at the respective nodes (see materials and methods).

**Table 3**

Coding for reconstructions of ancestral leaf anatomical characters, photosynthetic type and biogeography in Sesuvioideae. Coding of distribution area: A = Africa and Saudi Arabia, B = Australia, C = North and Middle America, D = South America and E = Asia. C3/C4 ("photosynthetic type"): 0 = C3/CAM; 1 = C4. Trait 1 "presence of water storage tissue (WST)": 0 = little or no WST; 1 = distinct WST. Trait 2 "presence of a hypodermis": 0 = not present, 1 = present. Trait 3 "position of kranz layer": 0 = absent, 1 = kranz layer around individual vascular bundles, 2 = continuous kranz layer around entire leaf. Trait 4 "shape of cross section": 0 = flat, 1 = round/rounded. Trait 5 "bladder cells": 0 = epidermis cells large or small but not bulging, 1 = large, bulging epidermis cells present. For illustration of anatomical types see Fig. 3.

Taxon	Distribution area	Photosyn. type	Anatomical type	C3/C4	Trait 1	Trait 2	Trait 3	Trait 4	Trait 5	Information on leaf anatomical character obtained from
<i>Phytolacca dioica</i> – outgroup	D	C3		0						Missing data
<i>Tetragonia tetragonoides</i>	A, B, C, D, E	CAM/C3		0						Missing data
<i>Aptenia cordifolia</i>	A	CAM/C3		0						Missing data
<i>Chryophyllum crystallinum</i>	A	CAM/C3		0	1	0	0	0	1	Kondo et al. (1998)
<i>Gibbaeum pachypodium</i>	A	CAM/C3		0						Missing data
<i>Delosperma cooperi</i>	A	CAM/C3		0	1	0	0	1	1	Konrad et al. (2013)
<i>Cypselea humifusa</i>	C	C4	Atriplicoid; NADP-ME	1	0	0	1	0	0	Muhaidat et al. (2007)
<i>Sesuvium congense</i>	A	C4	Portulacloid	1	1	0	1	1	1	Present study
<i>S. crithmoides</i>	A	C4	Pilosoid	1	1	0	1	1	1	Present study
<i>S. maritimum</i>	C	C3	Tribulocarpus type	0	1	0	0	0	1	Present study
<i>S. portulacastrum</i>	A, B, C, D, E	C3	Sesuvium portula castrum type, Tribulocarpus type	0	1	0	0	0	0	Present study
<i>S. sessile</i>	C	C3	Tribulocarpus type	0	1	0	0	0	1	Present study
<i>S. sesuvioides</i> (incl. <i>S. hydaspicum</i> , <i>S. nyasicum</i> ) <sup>a</sup>	A	C4	Portulacloid	1	1	0	1	0	0	Present study
<i>S. verrucosum</i>	C, D	C3	Tribulocarpus type	0	1	0	0	0	1	Present study
<i>Trianthema argentina</i>	D	C4		1						Missing data
<i>T. ceratosepala</i>	A	C3	Tribulocarpus type	0	0	0	0	0	0	Present study
<i>T. clavata</i>	B	C4		1						Missing data
<i>T. compacta</i>	B	C4		1						Missing data
<i>T. corallicola</i>	A	C4	Salsoloid	1	1	0	2	1	0	Present study
<i>T. corymbosa</i>	A	C4	Salsoloid	1	1	1	2	1	0	Present study
<i>T. crystallina</i>	A	C4	Atriplicoid	1	0	1	1	0	1	Present study
<i>T. megasperma</i>	B	C4		1						Missing data
<i>T. oxyacalyptra</i>	B	C4		1						Missing data
<i>T. parvifolia</i>	A	C4	Salsoloid	1	1	1	2	1	0	Present study
<i>T. patellitecta</i>	B	C4		1						Missing data
<i>T. pilosa</i>	B	C4	Atriplicoid	1	0	1?	1	?	0	Carolin et al. (1978)
<i>T. portulacastrum</i>	A, B, C, D, E	C4	Atriplicoid; NADP-ME and PEP-CK	1	0	0	1	0	0	Muhaidat et al. (2007), Muhaidat and McKown (2013)
<i>T. rhynchocalyptra</i>	B	C4		1						Missing data
<i>T. salsoloides</i>	A	C4	Salsoloid	1	1	1	2	1	0	Present study
<i>T. sedifolia</i>	A, B, E	C4	Portulacloid	1	1	1	1	1	0	Present study
<i>T. sheilae</i>	A	C4	Atriplicoid; NAD-ME	1	0	1	1	0	1	Present study, Muhaidat and McKown (2013)
<i>T. transvaalensis</i>	A	C4	Salsoloid	1	1	1	2	1	0	Present study
<i>T. turgidifolia</i>	B	C4		1						Missing data
<i>T. ufoensis</i>	B	C4		1						Missing data
<i>T. vleiensis</i>	A	C4	Salsoloid	1	1	1	2	1	0	Present study
<i>Tribulocarpus dimorphanthus</i>	A	C3	Tribulocarpus type	0	1	0	0	0	1	Present study
<i>T. retusus</i>	A	C3	Tribulocarpus type	0	1	0	0	0	1	Present study
<i>Zaleya galericulata</i>	B	C4	Atriplicoid	1	0	1	1	0	0	Carolin et al. (1978)
<i>Z. pentandra</i>	A	C4	Atriplicoid; NAD-ME and PEP-CK	1	0	1	1	0	0	Present study, Muhaidat et al. (2007), Muhaidat and McKown (2013)
<i>Z. redimita</i>	A	C4		1						Missing data

<sup>a</sup> A separation of *S. hydaspicum* and *S. nyasicum* sensu Gonçalves from *S. sesuvioides* (Gonçalves, 1965) is not supported by molecular or anatomical data in our study, and at this point we fail to see consistent morphological differences between these three species, but a closer investigation of the African species of *Sesuvium* is needed.

### $\delta^{13}\text{C}$ isotope analysis

$\text{C}_3$  species typically exhibit carbon isotope ratios of  $-22\text{\textperthousand}$  to  $-30\text{\textperthousand}$ , while  $\text{C}_4$  species exhibit  $-9\text{\textperthousand}$  to  $-15\text{\textperthousand}$  (Farquhar et al., 1989). Carbon isotope analysis showed that *Cypselea* ( $\delta^{13}\text{C} -11.5\text{\textperthousand}$ ) and *Zaleya* ( $\delta^{13}\text{C} -12.9\text{\textperthousand}$  to  $-13.7\text{\textperthousand}$ ) have  $\delta^{13}\text{C}$  values indicative of  $\text{C}_4$  photosynthesis, as well as all but one species of *Trianthema* (Table 4; online supplemental Table 2). The exception is *T. ceratosepala* Volkens & Irmsch. which expresses a  $\text{C}_3$  isotopic value of  $-24.6\text{\textperthousand}$ . In *Sesuvium*, four (*Sesuvium congense*, *Sesuvium crithmoides*, *Sesuvium mesembryanthemoides*, *S. sesuvioides*) of the 12

species expressed  $\text{C}_4$ -like  $\delta^{13}\text{C}$  values, while 7 exhibited exclusively  $\text{C}_3$ -like values. Of particular note is *Sesuvium edmonstonei* Hook. f., which has an intermediate  $\delta^{13}\text{C}$  value of  $-21.5\text{\textperthousand}$  that may indicate significant activity of PEP-carboxylase.

### Leaf anatomy

#### General leaf characters

Leaf blades vary in size and range from tiny (c. 5–8 mm in length and c. 4–5 mm in width in *Cypselea*) to relatively large (up to 70 mm long and c. 10 mm wide) in *S. crithmoides* Welw.

**Table 4**

Mean  $\delta^{13}\text{C}$  values of 39 species of Sesuvioideae. Detailed information for each sample can be found in supplemental Table 2. C<sub>3</sub>-like  $\delta^{13}\text{C}$  in bold. N = number of samples measured for the respective species.

Taxon	Mean $\delta^{13}\text{C}$ value
<b>Cypselea</b>	
<i>C. humifusa</i> Turpin	–11.5 (N=4)
<b>Sesuvium</b>	
<i>S. ayresii</i> Marais	<b>–25.6</b> (N=2)
<i>S. congeste</i> Welw. Ex Oliv.	–13.3 (N=1)
<i>S. crithmoides</i> Welw.	–12.2 (N=2)
<i>S. dystylum</i> Ridl.	<b>–27.6</b> (N=1)
<i>S. edmonstonei</i> Hook. f.	<b>–21.5</b> (N=2)
<i>S. maritimum</i> Britton, Stern & Pogggenb.	<b>–27.7</b> (N=5)
<i>S. mesembryanthemoides</i> Wawra & Peyr.	–11.2 (N=2)
<i>S. microphyllum</i> Willd.	<b>–25.7</b> (N=2)
<i>S. portulacastrum</i> L.	<b>–25.3</b> (N=7)
<i>S. sessile</i> Pers.	<b>–24.8</b> (N=3)
<i>S. sesuvioides</i> Verdc. (incl. <i>S. hydaspicum</i> (Edgew.) Gonc. and <i>S. nyasicum</i> (Baker) Gonc.) <sup>a</sup>	–12.4 (N=13)
<i>S. verrucosum</i> Raf. (incl. <i>S. erectum</i> Corr.)	<b>–24.8</b> (N=8)
<b>Trianthema</b>	
<i>T. argentina</i> Hunz. & Cocucci	–10.1 (N=1)
<i>T. ceratosepala</i> Volkens & Irmsch.	<b>–24.6</b> (N=3)
<i>T. compacta</i> C.T. White	–14.1 (N=1)
<i>T. corallicola</i> H.E.K. Hartmann & Liede	–14.6 (N=1)
<i>T. corymbosa</i> (Sonder) H.E.K. Hartmann & Liede	–13.5 (N=2)
<i>T. crystallina</i> (Forssk.) Vahl	–14.0 (N=2)
<i>T. cussackiana</i> F. Muell.	–10.8 (N=1)
<i>T. glossostigma</i> F. Muell.	–12.1 (N=2)
<i>T. hecatandra</i> Wingf. & M.F. Newman	–12.6 (N=2)
<i>T. monogyna</i> L.	–11.9 (N=2)
<i>T. oxyacalypta</i> F. Muell.	–13.2 (N=3)
<i>T. parvifolia</i> Mey. ex Sond.	–13.7 (N=2)
<i>T. pilosa</i> F. Muell.	–12.4 (N=2)
<i>T. portulacastrum</i> L.	–12.3 (N=4)
<i>T. rhynchosalypta</i> F. Muell.	–11.9 (N=2)
<i>T. salsoloides</i> Fenzl ex Oliv.	–12.3 (N=2)
<i>T. sedifolia</i> Viv.	–12.5 (N=3)
<i>T. transvaalensis</i> Schinz	–12.4 (N=1)
<i>T. turgidifolia</i> F. Muell.	–11.8 (N=1)
<i>T. ufoensis</i> H.E.K. Hartmann & Liede	–10.9 (N=1)
<i>T. vleiensis</i> H.E.K. Hartmann & Liede	–14.4 (N=2)
<b>Tribulocarpus</b>	
<i>Tr. dimorphantus</i> (Pax) S. Moore	–24.2 (N=1)
<b>Zaleya</b>	
<i>Z. decandra</i> (L.) Burm.f.	–10.8 (N=1)
<i>Z. galericulata</i> Eichler	–13.7 (N=3)
<i>Z. pentandra</i> (L.) C. Jeffrey (incl. <i>Z. govindia</i> Nair)	–12.9 (N=6)
<i>Z. redimita</i> (Melv.) H.E.K. Hartmann	–13.2 (N=1)
<i>Z. sennii</i> (Chiov.) C. Jeffrey	–13.2 (N=1)

<sup>a</sup> A separation of *S. hydaspicum* and *S. nyasicum* sensu Gonçalves from *S. sesuvioides* (Gonçalves, 1965) is not supported by molecular or anatomical data in our study, and at this point we fail to see consistent morphological differences between these three species, but a closer investigation of the African species of *Sesuvium* is needed.

and *S. portulacastrum*. Leaves are generally entire, and mostly moderately to strongly succulent. Leaf anatomy might show a dorsiventral, isobilateral, or centric symmetry. The common peripheral vascular bundles (VB) always have their xylem facing outwards. The epidermis (EPI) consists of equal or unequal, medium to large-sized cells which often form large bladder cells. Stomata are equally distributed on both surfaces. Leaf anatomy is variable, with many species showing a non-chlorenchymatous subepidermal cell layer (hypodermis = HYP), a distinct water storage tissue (WST) and multi-layered chlorenchyma (CHL). In order to classify leaf anatomical types, we followed previous schemes presented for C<sub>4</sub> eudicots in general (Edwards and Voznesenskaya, 2011; Muhaidat et al., 2007) and the Camphorosmeae (Freitag and Kadereit, 2013). As in Freitag and Kadereit (2013), we gave priority to (1) anatomical

features associated with C<sub>3</sub> and C<sub>4</sub> photosynthesis, (2) arrangement of vascular bundles, and (3) structure of the chlorenchyma.

#### C<sub>3</sub> leaf types (Figs. 3A–F and 4A)

**Tribulocarpus type (Fig. 3A–D).** Diagnostic character: all VB in one plane in the centre of the leaf. Description: leaves flat or biconvex, some slightly succulent with a central WST. In some species, the WST is present between veins only; CHL in 2–3 layers consisting of relatively small cells, CHL cells palisade-like on the upper side of the leaf and more rounded on the lower side of the leaf. EPI cells are large and often inflated to form large rounded bladder cells (e.g. *Sesuvium verrucosum* Raf., *Tribulocarpus*), HYP absent. The BS cells appear empty, with no obvious aggregation of organelles in a centripetal position. Occurrence: *Tribulocarpus dimorphantus* S. Moore, *Tribulocarpus retusus* (Thulin) Thulin & Liede, *Trianthema ceratosepala*, *S. edmonstonei*, *S. maritimum* (Walter) Stern, Britton & Pogggenb., *S. portulacastrum*, *S. sessile* Pers., *S. verrucosum*.  $\delta^{13}\text{C}$  value: –24.2 to –27.7.

**S. portulacastrum type (Fig. 3E and F).** Diagnostic character: three main VB in one plane in the centre of the leaf, numerous lateral VB at the periphery of the central WST. Description: leaves biconvex to terete, distinctly succulent with a central WST, CHL in 3–4 layers consisting of palisade-like cells on both sides of the leaf, EPI cells small, HYP absent. BS lacking organelle aggregations. Occurrence: *Sesuvium microphyllum* Willd., *S. portulacastrum*.  $\delta^{13}\text{C}$  value: –25.3 to –25.7.

#### C<sub>4</sub> leaf types (Figs. 3G–N and 4A)

**Atriplicoid type (Fig. 3G and H; Muhaidat and McKown, 2013; Fig. 1).** Diagnostic character: VB in a median plane, each with arcs of BS and palisade cells leaving a gap on the abaxial side, WST lacking. Description: leaves ± flat, non-succulent or succulent by large bladder cells; VB arranged in one line; CHL consisting of (1) an arc-like sheath of kranz cells around each bundle, (2) a palisade layer engirdling the kranz layer, (3) spongy-like parenchyma containing few chloroplasts filling the gaps, especially on the abaxial side; WST absent; HYP present or rarely absent (*C. humifusa* Turpin); EPI bladder cells large. Occurrence: *C. humifusa* (Muhaidat et al., 2007; Fig. 2), *Trianthema crystallina*, *T. portulacastrum*, *T. sheilae*, *Z. pentandra* (latter three see also Muhaidat and McKown, 2013; Fig. 1).  $\delta^{13}\text{C}$  value: –11.5 to –13.9.

**Salsoloid type (Fig. 3I and J).** Diagnostic character: CHL located at the periphery of a central WST consisting of continuous layers of kranz and mesophyll cells, a large central VB in the water storage tissue, numerous smaller VB at the periphery of the WST. Description: leaves ± terete, succulent; one large central VB, numerous lateral VB located in the WST or at the edge of the WST; CHL continuous (e.g., *Trianthema corymbosa* (Sonder) H.E.K. Hartmann & Liede, *Trianthema parvifolia* E. Meyer ex Sonder) or with a small to large gap at the abaxial side of the leaf (e.g., *Trianthema corallicola* H.E.K. Hartmann & Liede, *Trianthema salsoloides* Fenzl. ex Oliv., *Trianthema transvaalensis* Schinz, *Trianthema vleiensis* H.E.K. Hartmann & Liede), CHL consisting of a kranz layer and a palisade layer; HYP present, rarely absent (*T. corallicola*); EPI no or low bladder cells. Occurrence: *T. corallicola*, *T. corymbosa*, *T. parvifolia*, *T. salsoloides*, *T. transvaalensis*, *T. vleiensis*.  $\delta^{13}\text{C}$  value: –12.3 to –14.6.

#### Portulacelloid type (Fig. 3K and L)

Diagnostic character: CHL only on the adaxial (upper) side, ±equal-sized VB in one plane/arc on the adaxial side of the leaf, WST on the abaxial (lower) side, kranz cells forming open arcs. Description: leaves flat or almost terete, curved towards the abaxial side, slightly to distinctly succulent, mesophyll in 1–3 layers consisting

of palisade-like cells becoming more rounded towards the WST, the bundle sheath (BS) consisting of 5–8 kranz cells surrounding the adaxial (xylem) side of the vascular bundle but shows a gap on the abaxial (phloem) side, here the VB has direct contact to WST, HYP absent, EPI cells are large but no bladder cells. Occurrence: *S. sesuviooides*, *T. sedifolia* (sparse bladder cells).  $^{13}\text{C}$  value: −10.2 to −15.3. Notes: 1. The Portulacelloid type as described by Edwards and Voznesenskaya (2011) shows a complete wreath of kranz cells; kranz cells here form open arcs. 2. The leaves of *S. congeste* Welw. ex Oliv. differ from the type described here in showing a large central VB additionally to the smaller VB at the adaxial (upper) side of the leaf. 3. In some species (e.g., *S. sesuviooides*) the ratio of mesophyll to kranz cells is relatively high (c. 2.5:1). 4. Due to the lack of conclusive evidence for the separation of these species as suggested by Gonçalves (1965), we included *Sesuvium hydaspicum* (Edgew.) Gonc. and *Sesuvium nyasicum* (Baker) Gonc. in *S. sesuviooides*, but this species complex needs further investigations.

#### Pilosoid type (Fig. 3M and N)

**Diagnostic character:** CHL forms a closed ring at the leaf periphery surrounding a large WST, circular arrangement of small VB around the periphery of the leaf, main vein(s) in the centre of the WST, BS forming a full circle. **Description:** leaves round, succulent, mesophyll in one layer consisting of palisade-like cells forming a wreath-like structure on the outer and lateral sides of the VB, mesophyll mostly absent on the inner side of the VB, BS consisting of 5–7 cells that form a full circle, on the inner side of the VB these are in direct contact with WST, EPI cells large, forming bladder cells. Occurrence: *S. crithmoides*.  $^{13}\text{C}$  value: −12.2.

#### Ancestral state reconstruction using ML optimization

For all traits the log likelihood scores for both models tested were not significantly different at the  $p < 0.05$  level. Therefore, the simpler One-parameter Markov-k-state model was selected for the ancestral state reconstruction.

Trait 0 – photosynthetic type: when photosynthetic pathway is coded as a binary character with  $\text{C}_3$  or  $\text{C}_4$  as the two character states, the most likely scenario according to the ML optimization is a shift from  $\text{C}_3$  photosynthesis to  $\text{C}_4$  photosynthesis in the common ancestor of *Trianthema*, *Sesuvium* and *Zaleya* (Fig. 2). A reversal back to the  $\text{C}_3$  pathway would then be indicated in the ancestor of the American *Sesuvium* species (excluding *Cypselea*) and in the ancestor of *T. ceratosepala*.

Trait 1 – water storage tissue (Fig. 4B): The proportional likelihoods (PL) are equivocal for presence or absence of a distinct water storage tissue at the crown node of Sesuvioideae (PL for presence of WST = 0.72) and the crown nodes of *Trianthema* (PL for presence of WST = 0.62) and the *Sesuvium/Zaleya* clade (PL for presence of WST = 0.64). *Trianthema* subgenus *Papularia* is ancestrally succulent (PL for presence of WST = 0.98) and a loss of a WST occurred in the common ancestor of *T. sheilae* and *T. crystallina*. Notably these two species show very large bladder cells. The common ancestor of *Sesuvium* and *Cypselea* also was reconstructed to have a distinct WST (PL for presence of WST = 0.91) which then was lost in *Cypselea*.

Trait 2 – hypodermis (Fig. 4B): Reconstruction of the presence or absence of a hypodermis was equivocal at basal nodes in Sesuvioideae (crown node of the subfamily with PL for absence of HYP = 0.74). The ancestor of *Sesuvium* (incl. *Cypselea*) clearly lacked a hypodermis (PL for absence of HYP = 0.99) while the ancestor of *Zaleya* and *Trianthema* subgenus *Papularia* possessed a HYP (both PL = 0.99 for presence of HYP). Within *Trianthema* subgenus *Papularia*, the hypodermis was lost in *T. corallicola*.

Trait 3 – position of the  $\text{C}_4$  kranz layer (Fig. 4B): If the ancestor of *Trianthema*, *Sesuvium* and *Zaleya* was a  $\text{C}_4$  plant, it likely showed

kranz cells that surrounded individual vascular bundles (PL = 0.84). Only in the ancestor of *Trianthema* subgenus *Papularia* there is a shift towards a continuous kranz layer (PL for continuous kranz layer 0.9) and two subsequent reversals to kranz layers around individual bundles in *T. sedifolia* and the common ancestor of *T. sheilae* and *T. crystallina*.

Trait 4 – leaf shape (Fig. 4B): Ancestrally, the Sesuvioideae possessed flat leaves (PL = 0.96) and there are three shifts towards terete leaves, in (1) *S. crithmoides*, (2) *S. congeste* and (3) the ancestor of *Trianthema* subgenus *Papularia* (PL 0.95). In *Trianthema* subgenus *Papularia* there is a reversal to flat leaves in the common ancestor of *T. sheilae* and *T. crystallina*.

Trait 5 – bladder cells (Fig. 4B): Due to the scattered distribution of species with bulging bladder cells in the tree, the ancestral condition was reconstructed to be equivocal along the internal branches. For the position of species with bulging bladder cells compare Fig. 4.

## Discussion

### Phylogeny and biogeography of Sesuvioideae

In our analysis, the small genus *Tribulocarpus* is sister to all other Sesuvioideae which supports previous findings (Thiede, 2004; Thulin et al., 2012). *Tribulocarpus* consists of two species, one of which (*T. dimorphanthus*) is disjunctively distributed in southwestern and north-eastern Africa while the other (*T. retusus*) is endemic to Somalia (Thulin et al., 2012: Fig. 3). The two species differ in inflorescence and fruit morphology and represent a progenitor-derivative species pair in which *T. retusus* is derived from north-eastern populations of *T. dimorphanthus* (Thulin et al., 2012). The sister clade of *Tribulocarpus* consists of two major subclades: 1. *Trianthema* clade and 2. the *Zaleya/Sesuvium* (incl. *Cypselea*) clade. This *Trianthema/Zaleya/Sesuvium* lineage differs from *Tribulocarpus* in having circumscissile capsules. This clade was well-supported in previous studies (Thulin et al., 2012); however, the internal relationships remained unclear, in particular, the position of *Zaleya*. Our phylogenetic analysis supports a monophyletic *Trianthema* with the two currently recognized subgenera (*T. subgenus Trianthema* and *T. subgenus Papularia*) forming distinct monophyletic groups (Fig. 2). The inclusion of *Cypselea* in *Sesuvium* and the existence of two independent *Sesuvium* lineages, indicated already in Thulin et al. (2012), is confirmed. *Zaleya*, however, switches position from sister to *Trianthema* in Thulin et al. (2012) to sister of *Sesuvium + Cypselea* in the current analysis.

The centre of species diversity of Aizoaceae clearly lies in southern Africa with 96% of the species endemic to arid or semiarid parts of southern Africa (Chesselet et al., 2000). Most of these species arose from the extensive Miocene speciation within the subfamilies of the Aizoaceae that are sister to the Sesuvioideae (Klak et al., 2004). Further regions with high diversity of Aizoaceae are arid Eastern Africa and arid Australia (Hartmann, 1993). The subfamily Sesuvioideae originated in Africa/Arabia with three subsequent dispersal events to Australia and two to America (Fig. 2). As supported by the Afro-Arabian occurrence of *Tribulocarpus* and most *Trianthema/Zaleya/Sesuvium* species, the ancestor of the *Trianthema/Zaleya/Sesuvium* lineage clearly lived in Africa/Arabia (Fig. 2). *Trianthema* subgenus *Papularia* includes mainly species from arid to semi-arid regions of Africa. However, two intercontinental dispersal events are found within this lineage, one to Australia (*T. clavata* and *T. ufoensis*) and one to South America (*T. argentina*). Apart from the 12 species sampled in this study, *Trianthema* subgenus *Papularia* contains five additional species (Hartmann et al., 2011). Three of these are also distributed in Africa (*T. sanguinea* Volkens & Irmsch., East Africa, *T. hereroensis*

Schinz, Namibia, and *T. mozambiquensis* H.E.K. Hartmann & Liede, Mozambique), and two South Asian species (*T. pakistanensis* H.E.K. Hartmann & Liede, in Pakistan and western India) and *T. triquetra* (eastern India, Thailand, Indonesia, Philippines). The latter two species might be of particular interest to reconstruct the geographic spread of the subgenus in greater detail.

Australia was also colonized by species from *T.* subgenus *Trianthemoides* (Fig. 2), as indicated by the sister-relationship of East African *T. ceratosepala* with a speciose Australian clade. We were unable to include three Australian species, *T. cypseloidea* (Fenzl) Benth., *T. glossostigma* F. Muell., and *T. cussackiana* F. Muell. due to lack of material, but assume from capsule morphology that these belong to *T.* subgenus *Trianthemoides*. Subgenus *Trianthemoides* also includes a cosmopolitan species, *T. portulacastrum*, which is sister to all other species of the subgenus. So far, the evolutionary history and the area of origin of *T. portulacastrum* are unknown. The plant is known as an aggressive weed, especially in Thailand, Australia and South America. Its roots are also used medicinally in Asia (Aquilari, 2001).

The second subclade of the *Trianthemoides/Zaleya/Sesuvium* lineage consisting of the sister groups *Zaleya* and *Sesuvium* also shows intercontinental dispersal events. Within *Zaleya*, Australia was colonized by ancestors of the modern *Z. galericulata*, which is now widely distributed in arid Australia (Prescott and Venning, 1984). Within *Sesuvium*, there are two clades, one in Africa and the second in the Americas. The latter also includes *Cypselea humifusa*, which occurs on mudflats of receding ponds, lakes, canals and rivers from the West Indies to Mexico, Florida and the western USA (Ferren, 2003). Tree topology suggests that the American lineage reached North and Central America first (Fig. 2). Only few species such as *S. verrucosum* and *S. portulacastrum* expanded their distribution range to South America (specimen for *S. portulacastrum* e.g. Panigatti 444, Trinta and Fromm 534; for *S. verrucosum* Zimmerman 2156). *S. portulacastrum* is a cosmopolitan species often found on marine shorelines in the tropics and subtropics (Lonard and Judd, 1997; Ramani et al., 2006). This halophyte is easily distributed via sea currents and grows from washed up vegetative fragments (Lonard and Judd, 1997). Since *S. portulacastrum* tolerates salinity as well as

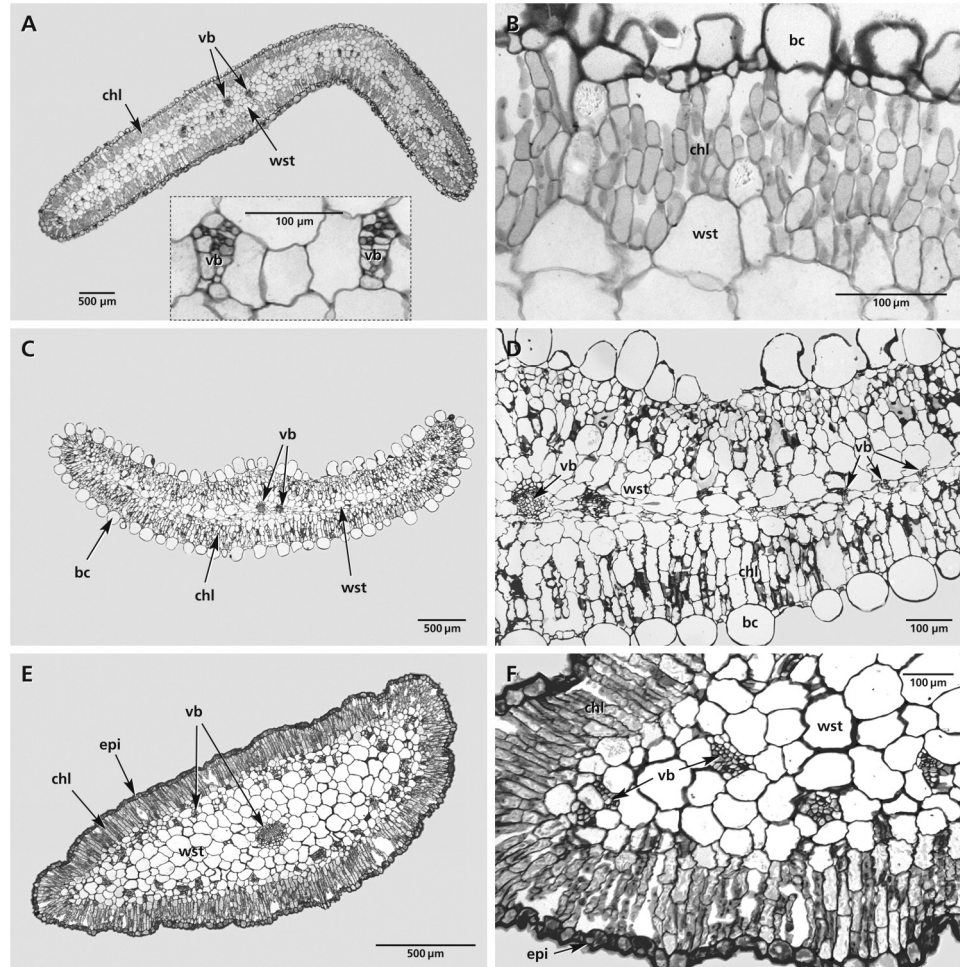


**Fig. 3.** Cross sections of two C<sub>3</sub> and four C<sub>4</sub> leaf anatomical types of Sesuvioideae. (A)–(D) *Tribulocarpus* type (C<sub>3</sub> leaves with all bundles in a central plane, central water storage tissue and distinct bladder cells), (A) and (B) *Tribulocarpus retusus* (specimen: Thulin et al., 10511, UPS), (C) and (D) *Sesuvium verrucosum* (specimen: K. Bohley, s.n., MJG); (E) and (F) *Sesuvium portulacastrum* type (multiple lateral vascular bundles at the periphery of the large central water storage tissue, no bladder cells), *Sesuvium portulacastrum* (specimen: P.H. Raven, 28497, MO); (G)–(N) C<sub>4</sub> leaf types. (G) and (H) Atriplicoid type (all bundles in a central plane, each with an arc of BS and palisade cells, no water storage tissue), *Trianthemoides crystallina* (specimen: Thulin et al., 9511, UPS); (I) and (J) Salsoloid type (large central WST, CHL in periphery of WST consisting of continuous layers of kranz and palisade cells), *Trianthemoides parvifolia* (specimen: Hartmann et al., 25483, HBG); (K) and (L) Portulaceloid type (CHL only on the adaxial side, all VB in one plane/arc on adaxial side, WST on the abaxial side, incomplete BS), *Trianthemoides sedifolia* (specimen: Thulin et al., 9684, UPS); (M) and (N) Pilosoid type (closed ring of CHL surrounding a large central WST, circular arrangement of VB with complete BS), *S. crithmoides* (specimen: Winter, 7786, PRE). *Sesuvium verrucosum* and *S. portulacastrum* were sectioned from fresh material while all other sections were made using herbarium material.

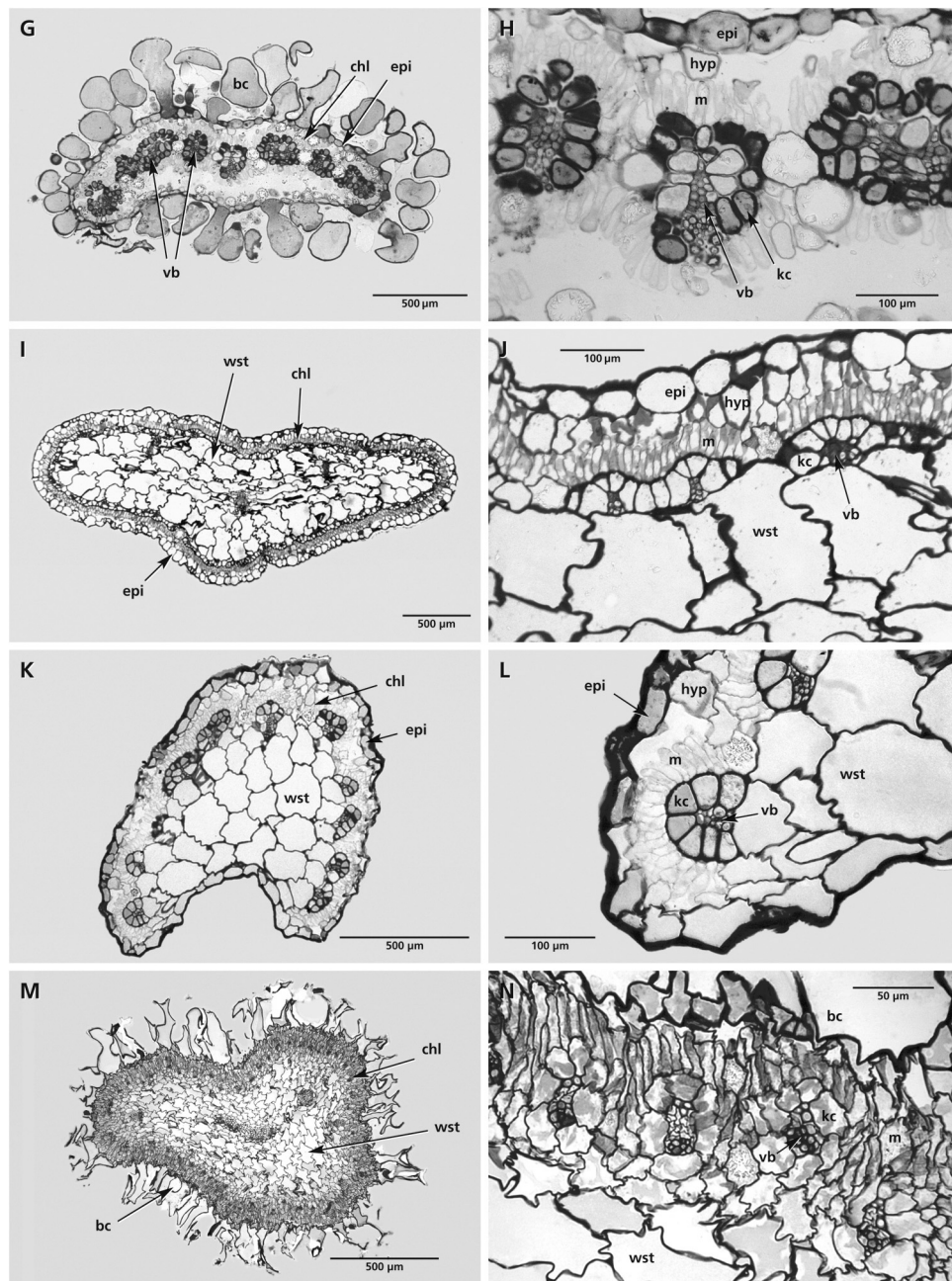


Fig. 3. (Continued).

toxic metals, it is of growing interest for the phytoremediation of contaminated soil (Patil et al., 2012).

#### Diversity of leaf anatomy in Sesuvioideae and rapid, multiple shifts of anatomical types

Sesuvioideae show two C<sub>3</sub> leaf types which differ in position of the vascular bundles – the *Tribulocarpus* type (bundles in one plane, Fig. 3A–D; see also Melo-de-Pinna et al., 2014: Fig. 5E and F) and *S. portulacastrum* type (bundles at the periphery of the water storage tissue; Fig. 3E and F). All C<sub>3</sub> leaves show a multi-layered chlorenchyma and lack a hypodermis. The amount of water storage tissue varies considerably and seems to be phenotypically plastic in some species (K. Bohley, pers. obs. for *S. portulacastrum*). *T. ceratosepala* for example lacks distinct water storage tissue but shows

large parenchyma cells between the veins. The lack of distinct BS cells with organelle aggregations in a centripetal position indicates that there is no anatomically C<sub>3</sub>–C<sub>4</sub> intermediate type in the Sesuvioideae species examined (Sage et al., 2014). Only the intermediate δ<sup>13</sup>C value in *S. edmonstonei* from the Galapagos Islands (−21.5‰) indicates that in this species a carbon concentrating mechanism could operate. However, the leaf anatomy does not give any indication of C<sub>3</sub>/C<sub>4</sub>-intermediacy (online supplement Fig. 1). High δ<sup>13</sup>C values near −21‰ can occur in C<sub>3</sub> plants if stomatal conductance is very low relative to photosynthesis (Sage and Kubien, 2007). Unfortunately, the herbarium material was degraded to a degree that we could not get DNA, but we assume that this species is closely related to the *S. portulacastrum* group.

The atriplicoid type of kranz anatomy has been reported to be the common type in Sesuvioideae (Carolin et al., 1978; Muhaidat

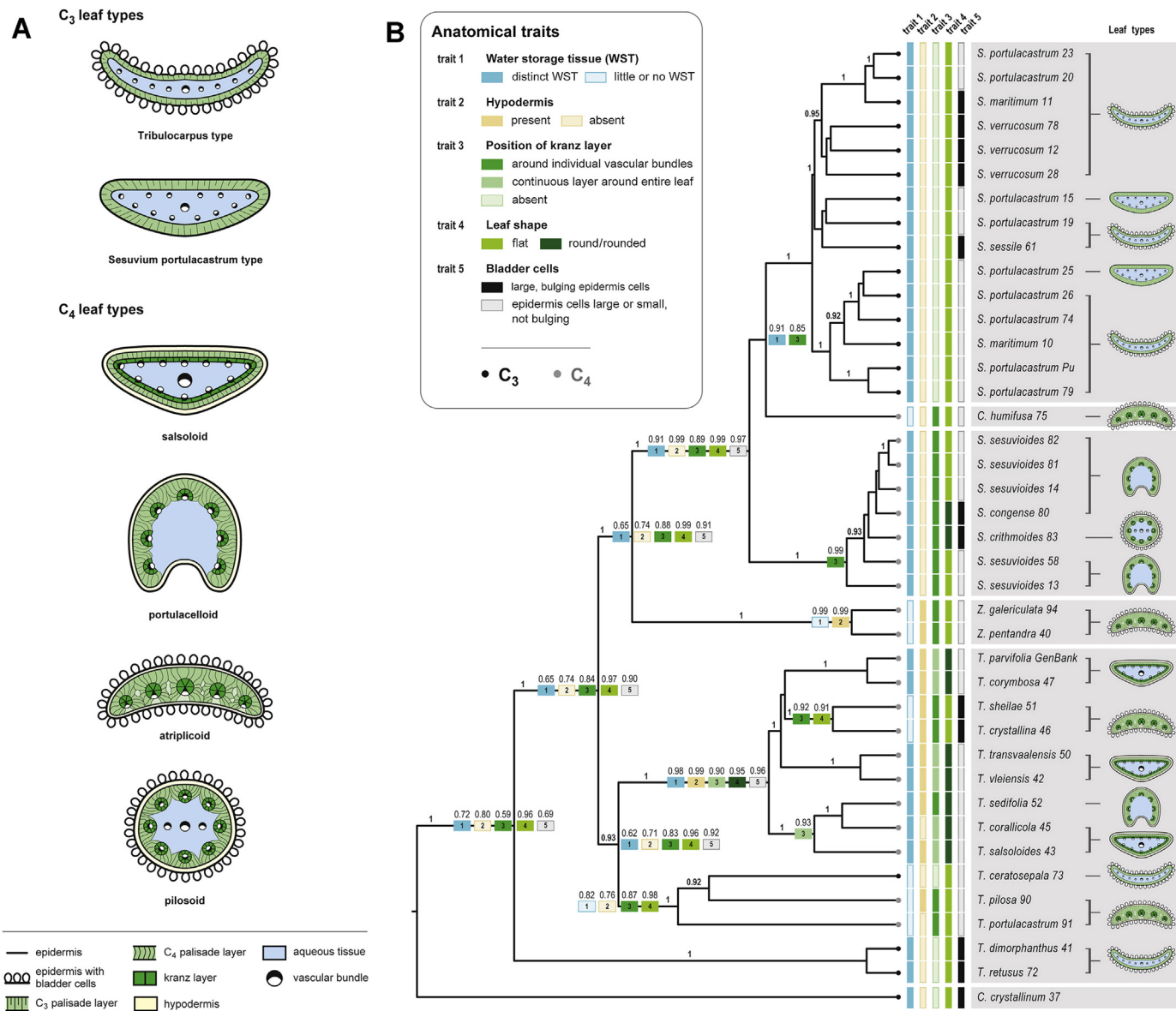


**Fig. 4.** Evolution of leaf anatomy in Sesuvioideae. (A) Schematic illustration of C<sub>3</sub> and C<sub>4</sub> leaf types. (B) Ancestral character state reconstructions of five leaf traits using maximum likelihood optimization. Proportional likelihoods for character states are given for selected nodes and mapped on the MCC tree resulting from the BEAST analysis of a slightly reduced taxon set (39 accessions representing 26 species and all genera of Sesuvioideae) because the data were not available for all species.

et al., 2007). However, according to our survey four C<sub>4</sub> anatomical types are present in Sesuvioideae (atriplicoid in seven spp., salsoloid in six spp., portulacelloid in four spp. and pilosoid in one species). These show the major features of previously described leaf types of other C<sub>4</sub> groups (Table 3, Figs. 3 and 4A; compare Edwards and Voznesenskaya, 2011). While an atriplicoid leaf type is most common among C<sub>4</sub> plants (Sage et al., 2011) the other three types are more restricted in their occurrence and only found in distinctly succulent lineages. The salsoloid leaf type is common in the speciose Chenopodiaceae subf. Salsoloideae (Kadereit et al., 2003), the portulacelloid leaf type is only known from *Portulaca* section *Portulacella* (Portulacaceae; Ocampo et al., 2013; Voznesenskaya et al., 2010), while the pilosoid-leaf type is also found in *Portulaca* (*Pilosa* clade, Portulacaceae; Edwards and Voznesenskaya, 2011; Ocampo et al., 2013). Mapping the leaf types onto the phylogeny illustrates that they do not consistently correspond to the distinct subclades of Sesuvioideae, but occur in several lineages indicating that leaf anatomy can be altered with relative ease in Sesuvioideae (Fig. 4B).

Similar change of leaf anatomical characters was also found in the mostly succulent C<sub>4</sub> genus *Bassia* (Chenopodiaceae,) in which repeated loss of WST is associated with multiple origins of the atriplicoid leaf type from an ancestrally succulent C<sub>4</sub> leaf type (Freitag and Kadereit, 2013; Kadereit et al., 2014). In Sesuvioideae, a similar pattern can be observed (Fig. 4B). *T. crystallina* and *T. sheilae* show an atriplicoid leaf anatomy and reduced or absent WST. These two species are nested in a clade with ancestrally succulent leaves and closely related species mostly show a salsoloid and in one case a portulacelloid leaf type (Fig. 4B). Another example of loss of WST and shift to an atriplicoid-leaf type is *Cypselea* which is nested among strongly succulent species of *Sesuvium*. Further origins of the atriplicoid leaf type are found in *Zaleya* and *T. pilosa* and *T. portulacastrum*, however, in these lineages the ancestral states of WST are unclear.

In Sesuvioideae, salsoloid leaves which are characterized by a continuous layer of kranz cells around the water storage tissue and the vascular bundles are restricted to *Trianthema* subgenus *Papularia*, however, the subgenus also contains species with portulacelloid and atriplicoid leaf anatomy in derived positions. This indicates that also the position of the kranz layer (around individual bundles or around the entire leaf) might change rapidly in a lineage. In other succulent groups, however, distinct variation in kranz anatomy was found to be a signature of independent C<sub>4</sub> origins. In *Suaedoideae* four independent origins of C<sub>4</sub> are supported by phylogenetic and anatomical evidence (Rosnow et al., 2014; Schütte et al., 2003). In *Portulacaceae*, which exhibit a very similar range of anatomies as Sesuvioideae, including the atriplicoid, pilosoid and portulacelloid C<sub>4</sub> anatomy, these types clearly support monophyletic clades (Ocampo et al., 2013). However, this study and the study of Kadereit et al. (2014) show that there are also lineages in which shifts in overall leaf anatomy and in single anatomical traits are frequent and deeply nested in C<sub>4</sub> clades suggesting fast evolutionary change of leaf anatomical traits within C<sub>4</sub> lineages. In such groups distinct variation in kranz anatomy cannot evaluate hypotheses of independent or common C<sub>4</sub> origin. The examples of *Bassia* (Kadereit et al., 2014) and *Trianthema* subgenus *Papularia* clearly demonstrate that dense infrageneric sampling might reveal an unexpected diversity of leaf anatomy in C<sub>4</sub> lineages.

#### *Evolution of C<sub>4</sub> photosynthesis and leaf anatomy in Sesuvioideae*

The ML optimization favours the hypothesis of a single early gain of C<sub>4</sub> photosynthesis in the ancestor of the *Trianthema/Sesuvium/Zaleya* lineage and two subsequent losses, one in *Sesuvium* and one in *Trianthema* (Fig. 2). If this was true, the optimization of

individual leaf anatomical traits (Fig. 4B) suggests that the ancestor of C<sub>4</sub> – species in Sesuvioideae probably had flat C<sub>3</sub> leaves with a multi-layered chlorenchyma and no hypodermis. The presence of a distinct water storage tissue in the last C<sub>3</sub> ancestor is uncertain (although more likely than its absence; Fig. 4B). Also, the possession of kranz cells around individual bundles seems to be the ancestral state, followed by a shift to a Salsoloid type with a continuous kranz layer around the leaf periphery which may have occurred in the ancestor of *Trianthema* subgenus *Papularia* (Fig. 4B).

This conclusion of a single C<sub>4</sub> origin and two subsequent losses is surprising, however, given the presence of different biochemical subtypes in *Cypselea*, *Trianthema* and *Zaleya* (Muhammad et al., 2007; Muhammad and McKown, 2013), and the anatomical variability identified here. Also, reversals from C<sub>4</sub> back to C<sub>3</sub> are unlikely given the complexity of the C<sub>4</sub> trait (Christin et al., 2014, 2010). For these reasons, it is useful to consider alternative scenarios that do not allow reversals to C<sub>3</sub>. If reversals are not allowed, our results indicate that a minimum of six independent gains of C<sub>4</sub> photosynthesis have occurred (Fig. 2): (1) *Cypselea*, (2) *Zaleya*, (3) *T. portulacastrum*, (4) *Trianthema* subgenus *Papularia*, (5) *Trianthema* subgenus *Trianthema* (excl. *T. portulacastrum* and *T. ceratosepala*), (6) African species of *Sesuvium*.

Multiple C<sub>4</sub> origins appear to be unlikely and non-parsimonious; however, biochemical diversity of C<sub>4</sub> types in the Sesuvioideae might indicate non-homology of the C<sub>4</sub> syndrome. The biochemical subtype is only known for four of the C<sub>4</sub> species in Sesuvioideae, but indicates independent origins (Muhammad et al., 2007; Muhammad and McKown, 2013). The four types are: (1) *C. humifusa* NADP-ME, (2) *Z. pentandra* NAD-ME and PEP-CK, (3) *T. portulacastrum* NADP-ME and PEP-CK, (4) *T. sheilae* NAD-ME (*Trianthema* subgenus *Papularia*). These four species represent different C<sub>4</sub> lineages (lineage 1–4, see above and Fig. 4B). Independent origins of NADP-ME and NAD-ME are most probable because the two subtypes have many unique traits that are thought to be important for efficient function of each subtype (Dengler and Nelson, 1999; Kanai and Edwards, 1999; Sage et al., 2014). For example, in the NADP-ME subtype, the BS chloroplasts have greatly reduced levels of thylakoid stacking and PSII investment and the numbers of BS mitochondria are substantially different in the two subtypes and differ in their association with BS chloroplasts (Edwards et al., 2004). The respective ultrastructure and biochemistry of the two subtypes are uniquely complex and well integrated, such that switching between the two would entail not just the changeover of a decarboxylase and a couple of other enzymes, but the wholesale replacement of the subtype architecture. For this reason, the presence of distinct subtypes supports hypotheses of multiple origins.

We admit, however, that this argument is circumstantial, and additional evidence is needed to support the hypothesis of distinct origins and reject the possibility of reversions back to C<sub>3</sub>. One approach is to further examine the genome and anatomical structure for “ghost” signatures of previous C<sub>4</sub> function in the C<sub>3</sub> *Sesuvium* clade and in *T. ceratosepala*. Anatomically, ghost signatures might include vestiges of kranz anatomy such as enlarged BS with enhanced organelle numbers; neither was observed in the C<sub>3</sub> *Sesuvium* leaves examined. Genomically, ghost signatures may include C<sub>4</sub>-type residues left behind in the gene sequence of the C<sub>4</sub>-specific enzymes (Christin et al., 2010). Another approach could be the study of C<sub>4</sub> key enzymes and their adaptive amino acid changes to distinguish between multiple or a single recruitment of the enzymes from a C<sub>3</sub> ancestor (Christin et al., 2014; Rosnow et al., 2014). Such an approach has been used with PEP carboxylase to support the hypothesis of multiple C<sub>4</sub> origins over a reversion hypothesis in the *Portulaca* and *Mollugo* clades (Christin et al., 2014, 2011). In *Portulaca*, where both NAD-ME and NADP-ME lines have evolved early in the genus, the analysis of PEPCase indicates distinct

origins of three C<sub>4</sub> clades, which is also indicated by distinct kranz anatomies (Christin et al., 2014; Ocampo et al., 2013). A similar analysis for the Sesuvioideae in which numerous shifts in biochemical and anatomical C<sub>4</sub> traits seem to have occurred will be a valuable follow-up to this study and should provide clear evidence in favour of the multiple origin versus the reversal hypothesis.

Clarification of multiple origin versus reversal hypotheses will strongly affect hypotheses regarding where, when and under which environmental conditions C<sub>4</sub> photosynthesis arose in Sesuvioideae. If a single C<sub>4</sub> origin is assumed, it likely would have been in the Afro-Arabian region where the ancestor of the C<sub>4</sub> clades in *Zaleya*, *Sesuvium* and *Trianthema* is predicted to have occurred. If multiple origins are considered, the *Trianthema* subg. *Papularia* and the African *Sesuvium* clearly originated in Africa/Arabia. The presence of most species of C<sub>4</sub> *Sesuvium* in arid-to-semi-arid southern Africa indicates that C<sub>4</sub> arose here. This region also appears to be the centre of origin of numerous eudicot C<sub>4</sub> clades such as the C<sub>4</sub> lineages in *Anticharis* Endl., *Blepharis* Juss., *Gisekia* L., *Mollugo* L. and *Zygophyllum* L. (Bissinger et al., 2014 and ref. therein). All species of African species of *Sesuvium* are highly salt tolerant as is the case with their American C<sub>3</sub> relatives (excl. *Cypselea*). *Trianthema* subg. *Papularia* are found in open, dry to extremely dry habitats in disturbed places or on the coast. Only some species in this clade tolerate saline conditions and are found in coastal plains or upper edges of salt pans (Hartmann et al., 2011). If *Trianthema* subg. *Trianthema* (excl. *T. portulacastrum* and *T. ceratosepala*) turns out to be an independent origin of C<sub>4</sub> it represents one of the rare C<sub>4</sub> origins of Australia (compare Fig. 2). The ancestral area of *T. portulacastrum* remains somewhat uncertain but is likely also Africa/Arabia. *Cypselea* is probably a distinct C<sub>4</sub> lineage arising in the West Indies or Mesoamerica, possibly from ancestral C<sub>3</sub> *Sesuvium* that dispersed across the Atlantic from Africa and is now extinct in Africa. *Cypselea* is currently found in widely separated wetland habitats, where it grows in mid-summer as a ruderal on the muddy shores of receding lakes and rivers (Ferren, 2003). Its disjunct occurrence across the northern Western Hemisphere indicates it can be dispersed over long-distances by water fowl (Sage, unpublished).

Examples of closely related CAM and C<sub>4</sub> lineages are relatively rare (Edwards and Ogburn, 2012). Apart from Aizoaceae, both carbon concentrating mechanisms (CCM) occur in Euphorbiaceae and Portulacineae. For Portulacineae, Christin et al. (2014) propose the multiple origin of the C<sub>4</sub> pathway via intermediate forms (as today found in *Portulaca cryptopetala* Speg.) from an ancestral CAM-like type in the ancestor of *Portulaca*. Sesuvioideae and their CAM relatives in the other subfamilies of Aizoaceae would be an ideal group to further investigate shared origins or precursors of key enzymes in CAM and C<sub>4</sub> plants as well as anatomical and ecological trajectories that favour one of the two CCMs over the other. C<sub>3</sub> species of *Sesuvium* with their derived position in an otherwise C<sub>4</sub> clade might be particularly interesting in this respect. Previous studies on *S. portulacastrum* showed unexpected increase in malate concentration and high activity of PEPC during the light period, which is interpreted as a reaction to increased salt concentrations with malate as counter-ion to Na<sup>+</sup> (Bhosale and Shinde, 1983; Ramani et al., 2006). On the other hand, some carbon concentrating mechanism cannot be ruled out with certainty, although δ<sup>13</sup>C isotopic values (see online supplemental Table 2) do not support full C<sub>4</sub> or obligate CAM.

## Acknowledgements

We thank the following herbaria AD, B, BOL, BONN, BRIT, C, CAS, DNA, HBG, K, LP, MEX, MO, NBG, PRE, S, TEX/LL, UPS, WAG, Z/WT for either loan of material and/or granting permission to extract DNA from leaf fragments. We are grateful to P. Winter (South African

National Biodiversity Institute (SANBI), Kirstenbosch) and D. Bellstedt (Univ. Stellenbosch) for material of African *Sesuvium* and *Trianthema*, respectively. We thank Isabell Rupp (Mainz) for her creative help with testing and inventing suitable staining methods. We thank our artists D. Franke and M. Geyer (Mainz) for their help with the illustrations and M. Maus (Mainz) for help with the isotope measurements. We are thankful for the constructive comments and criticisms of two anonymous reviewers and P. Endress (Zürich) which helped to improve the manuscript. Financial support for this study came from the German Science Foundation (grant to G. Kadereit, KA1816/7-1) and the Feldbauschstiftung (grant to G. Kadereit and K. Bohley for the study of *Sesuvium*).

## Appendix A. Supplementary data

Supplementary data associated with this article can be found, in the online version, at <http://dx.doi.org/10.1016/j.ppees.2014.12.003>.

## References

- Aquilar, N.O., 2001. In: Van Valkenburg, J.L.C.H., Bunyaphatsara, N. (Eds.), *Trianthema portulacastrum* L. [Web reference] Record from PROSEbase. PROSEA (Plant Resources of South-East Asia) Foundation, Bogor, Indonesia, <http://www.proseanet.org> (accessed 18.06.14).
- Bhosale, L.J., Shinde, L.S., 1983. Photosynthetic products and enzymes in a mangrove, *Aegiceras corniculatum* (L.) Blanco and a Halophyte, *Sesuvium portulacastrum* L.\*. *Photosynthetica* 17, 59–63.
- Bissinger, K., Khoshravesh, R., Kotrade, J.P., Oakley, J., Sage, T.L., Sage, R.F., Hartmann, H.E.K., Kadereit, G., 2014. *Gisekia* (Gisekiaceae): phylogenetic relationships, biogeography, and ecophysiology of a poorly known C<sub>4</sub> lineage in the Caryophyllales. *Am. J. Bot.* 101, 499–509, <http://dx.doi.org/10.3732/ajb.1300279>.
- Bittrich, V., 1990. *Systematic Studies in Aizoaceae*, 23b. Mitt. Inst. Allg. Bot., Hamburg, pp. 491–507.
- Bittrich, V., Hartmann, H.E.K., 1988. The Aizoaceae – a new approach. *Bot. J. Linn. Soc.* 97, 239–254.
- Bräutigam, A., Weber, A.P.M., 2011. Transport processes: connecting the reactions of C<sub>4</sub> photosynthesis. In: Raghavendra, A.S., Sage, R.F. (Eds.), *C<sub>4</sub> Photosynthesis and Related CO<sub>2</sub> Concentrating Mechanisms*. Springer, Dordrecht, The Netherlands, pp. 199–219.
- Carolin, R.C., Jacobs, S.W.L., Veski, M., 1978. Kranz cells and mesophyll in the Chenopodiaceae. *Aust. J. Bot.* 26, 683–698.
- Chesselet, P., Smith, G.F., Burgoynes, P.M., Klak, C., Hammer, S.A., Hartmann, H.E.K., Kurzweil, H., van Jaarsveld, E.J., van Wyk, B.-E., Leistner, O.A., 2000. *Mesembryanthemaceae*. In: Leistner, O.A. (Ed.), *Seed Plants of Southern Africa: Families and Genera*. Strelitzia, 10. National Botanical Institute, Pretoria, pp. 360–410.
- Christin, P.A., Freckleton, R.P., Osborne, C.P., 2010. Can phylogenetics identify C<sub>4</sub> origins and reversals? *Trends Ecol. Evol.* 25, 403–409, <http://dx.doi.org/10.1016/j.tree.2010.04.007>.
- Christin, P.A., Sage, T.L., Edwards, E.J., Ogburn, R.M., Koshravesh, R., Sage, R.F., 2011. Complex evolutionary transitions and the significance of C<sub>3</sub>–C<sub>4</sub> intermediate forms of photosynthesis in Molluginaceae. *Evolution* 65, 643–660, <http://dx.doi.org/10.1111/j.1558-5646.2010.01168.x>.
- Christin, P.A., Arakaki, M., Osborne, C.P., Bräutigam, A., Sage, R.F., Hibberd, J.M., Kelly, S., Covshoff, S., Wong, G.K.-S., Hancock, L., Edwards, E.J., 2014. Shared origin of a key enzyme during the evolution of C<sub>4</sub> and CAM metabolism. *J. Exp. Bot.*, <http://dx.doi.org/10.1093/jxb/eru087>.
- Dengler, N.G., Nelson, T., 1999. Leaf structure and development in C<sub>4</sub> plants. In: Sage, R.F., Monson, R.K. (Eds.), *C<sub>4</sub> Plant Biology*. Academic Press, San Diego, pp. 133–172.
- Downton, W.J.S., 1975. The occurrence of C<sub>4</sub> photosynthesis among plants\*. *Photosynthetica* 9, 96–105.
- Drummond, A.J., Ho, S.Y.W., Philips, M.J., Rambaut, A., 2006. Relaxed phylogenies and dating with confidence. *PLoS Biol.* 4, e88, <http://dx.doi.org/10.1371/journal.pbio.0040088>.
- Drummond, A.J., Rambaut, A., 2007. BEAST: Bayesian evolutionary analysis by sampling trees. *BMC Evol. Biol.* 7, 214, <http://dx.doi.org/10.1186/1471-2148-7-214>.
- Edwards, E.J., Ogburn, R.M., 2012. Angiosperm responses to a low-CO<sub>2</sub> world: CAM and C<sub>4</sub> photosynthesis as parallel evolutionary trajectories. *Int. J. Plant Sci.* 173, 724–733, <http://dx.doi.org/10.1086/666098>.
- Edwards, G.E., Franceschi, V.R., Voznesenskaya, E.V., 2004. Single-cell C<sub>4</sub> photosynthesis versus the dual-cell (kranz) paradigm. *Annu. Rev. Plant Biol.* 55, 173–196, <http://dx.doi.org/10.1146/annurev.arplant.55.031903.141725>.
- Edwards, G.E., Voznesenskaya, E.V., 2011. C<sub>4</sub> photosynthesis: kranz forms and single-cell C<sub>4</sub> in terrestrial plants. In: Raghavendra, A.S., Sage, R.F. (Eds.), *C<sub>4</sub> Photosynthesis and Related CO<sub>2</sub> Concentrating Mechanisms*. Springer, Berlin, pp. 29–61.
- Farquhar, G.D., Ehleringer, J.R., Hubick, K.T., 1989. Carbon isotope discrimination and photosynthesis. *Annu. Rev. Plant Physiol. Plant Mol. Biol.* 40, 503–537.

- Ferren Jr., W.R., 2003. *Cypselea*. In: Flora of North America Editorial Committee (Ed.), *Flora of North America*, vol. 4. Oxford University Press, Oxford, p. 82.
- Flowers, T.J., Colmer, T.D., 2008. Salinity tolerance in halophytes. *N. Phytol.* 179, 945963, <http://dx.doi.org/10.1111/j.1469-8137.2008.02531.x>.
- Forest, F., Chase, M.W., 2009. Eudicots. In: Hedges, S.B., Kumar, S. (Eds.), *The Timetree of Life*. Oxford University Press, Oxford, pp. 169–176.
- Freitag, H., Kadereit, G., 2013. C<sub>3</sub> and C<sub>4</sub> leaf anatomy types in Camphorosmeae (Camphorosmoideae/Chenopodiaceae). *Plant Syst. Evol.* 300, 665–687, <http://dx.doi.org/10.1007/s00606-013-0912-9>.
- Golenberg, E.M., Clegg, M.T., Durbin, M.L., Doebley, J., Ma, D.P., 1993. Evolution of a noncoding region of the chloroplast genome. *Mol. Phylogenetic Evol.* 2, 52–64.
- Gonçalves, M.L., 1965. Subsídios para o conhecimento da flora da Angola – I. Garcia de Orta 13, 379–382.
- Gouy, M., Guindon, S., Gascuel, O., 2010. SeaView Version 4: a multiplatform graphical user interface for sequence alignment and phylogenetic tree building. *Mol. Biol. Evol.* 27, 221–224.
- Hartmann, H.E.K., 1993. *Aizoaceae*. In: Kubitzki, K., Rohwer, J., Bittrich, V. (Eds.), *Flowering Plants Dicotyledons*. Springer, Berlin, Heidelberg, pp. 37–69.
- Hartmann, H.E.K., 2001a. *Illustrated Handbook of Succulent Plants: Aizoaceae A–E*. Springer, Heidelberg.
- Hartmann, H.E.K., 2001b. *Illustrated Handbook of Succulent Plants: Aizoaceae F–Z*. Springer, Heidelberg.
- Hartmann, H.E.K., Meve, U., Liede-Schumann, S., 2011. Towards a revision of *Trianthema*, the Cinderella of Aizoaceae. *Plant Ecol. Evol.* 144, 177–213.
- Hassan, N.S., Thiede, J., Liede-Schumann, S., 2005. Phylogenetic analysis of Sesuvioideae (Aizoaceae) inferred from nrDNA internal transcribed spacer (ITS) sequences and morphological data. *Plant Syst. Evol.* 255, 121–143.
- Jacobs, S.W.L., 2001. Review of leaf anatomy and ultrastructure in the Chenopodiaceae (Caryophyllales). *J. Torrey Bot. Soc.* 128, 236–253, <http://dx.doi.org/10.2307/3088716>.
- Kadereit, G., Borsch, T., Weising, K., Freitag, H., 2003. Phylogeny of Amaranthaceae and Chenopodiaceae and the evolution of C<sub>4</sub> photosynthesis. *Int. J. Plant Sci.* 164, 959–986.
- Kadereit, G., Ackery, D., Pirie, M.D., 2012. A broader model for C<sub>4</sub> photosynthesis evolution in plants inferred from the goosefoot family (Chenopodiaceae s.s.). *Proc. R. Soc. Lond. B* 279, 3304–3311, <http://dx.doi.org/10.1098/rspb.2012.0440>.
- Kadereit, G., Lauterbach, M., Pirie, M.D., Arafeh, R., Freitag, H., 2014. When do different C<sub>4</sub> leaf anatomies indicate independent C<sub>4</sub> origins? Parallel evolution of C<sub>4</sub> leaf types in Camphorosmeae (Chenopodiaceae). *J. Exp. Bot.*, <http://dx.doi.org/10.1093/jxb/eru169>.
- Kanai, R., Edwards, G.E., 1999. The biochemistry of C<sub>4</sub> photosynthesis. In: Sage, R.F., Monson, R.K. (Eds.), *C<sub>4</sub> Plant Biology*. Academic Press, San Diego, pp. 49–87.
- Klak, C., Khunou, A., Reeves, G., Hedderston, T., 2003. A phylogenetic hypothesis for the Aizoaceae (Caryophyllales) based on four plastid DNA regions. *Am. J. Bot.* 90, 1433–1445.
- Klak, C., Reeves, G., Hedderston, T., 2004. Unmatched tempo of evolution in Southern African semi-desert ice plants. *Nature* 427, 63–65, <http://dx.doi.org/10.1038/nature02243>.
- Kondo, A., Nose, A., Ueno, O., 1998. Leaf inner structure and immunogold localization of some key enzymes involved in carbon metabolism in CAM plants. *J. Exp. Bot.* 49, 1953–1961.
- Konrad, W., Flues, F., Schmich, F., Speck, T., Speck, O., 2013. An analytic model of the self-sealing mechanism of the succulent plant *Delosperma cooperi*. *J. Theor. Biol.* 336, 96–109, <http://dx.doi.org/10.1016/j.jtbi.2013.07.013>.
- Lonard, R.I., Judd, F.W., 1997. The biological flora of coastal dunes and wetlands. *Sesuvium portulacastrum* (L.) L. *J. Costal Res.* 13, 96–104.
- Maddison, W.P., Maddison, D.R., 2011. Mesquite: A Modular System for Evolutionary Analysis. Version 2.75 [computer program]. Available on the Internet at: <http://mesquitemproject.org>.
- Melo-de-Pinna, G.F.A., Ogura, A.S., Arruda, E.C.P., Klak, C., 2014. Repeated evolution of endoscopic peripheral vascular bundles in succulent leaves of Aizoaceae (Caryophyllales). *Taxon* 63, 1037–1052, <http://dx.doi.org/10.12705/635.8>.
- Muhaidat, R., McKown, A.D., 2013. Significant involvement of PEP-CK in carbon assimilation of C<sub>4</sub> eudicots. *Ann. Bot.-London* 111, 577–589.
- Muhaidat, R., Sage, R.F., Dengler, N.G., 2007. Diversity of Kranz anatomy and biochemistry in C<sub>4</sub> eudicots. *Am. J. Bot.* 94, 362–381.
- Ocampo, G., Koteyeva, N.K., Voznesenskaya, E.V., Edwards, E.E., Sale, T.L., Sage, R.F., Columbus, J.T., 2013. Evolution of leaf anatomy and photosynthetic pathways in Portulacaceae. *Am. J. Bot.* 100, 2388–2402, <http://dx.doi.org/10.3732/ajb.1300094>.
- Ogburn, R.M., Edwards, E.J., 2013. Repeated origin of three-dimensional leaf venation releases constraints on the evolution of succulence in plants. *Curr. Biol.* 23, 722–726, <http://dx.doi.org/10.1016/j.cub.2013.03.029>.
- Oxelman, B., Lidén, M., Berglund, D., 1997. Chloroplast rps16 intron phylogeny of the tribe Sileneae (Caryophyllales). *Plant Syst. Evol.* 206, 393–410.
- Patil, A.V., Lokhande, V.H., Suprasanna, P., Bapat, V.A., Jadhav, J.P., 2012. *Sesuvium portulacastrum* (L.) L.: a potential halophyte for the degradation of toxic textile dye, Green HE4B. *Planta* 235, 1051–1063, <http://dx.doi.org/10.1007/s00425-011-1556-z>.
- Popp, M., Oxelman, B., 2001. Inferring the history of the polyploid *Silene aegaea* (caryophyllaceae) using plastid and homoeologous nuclear DNA sequences. *Mol. Phylogenetic Evol.* 20, 474–481, <http://dx.doi.org/10.1006/mpev.2001.0977>.
- Prescott, A., Venning, J., 1984. *Aizoaceae*. In: Flora of Australia. Australian Government Publishing Service, Canberra, pp. 19–62.
- Raghavendra, A.S., Das, V.S.R., 1978. The occurrence of C<sub>4</sub>-photosynthesis: a supplementary list of C<sub>4</sub>-plants reported during late 1974 – Mid 1977\*. *Photosynthetica* 12, 200–208.
- Ramani, B., Reeck, T., Debez, A., Stelzer, R., Huchzermeyer, B., Schmidt, A., Papenbrock, J., 2006. *Aster tripolium* L. and *Sesuvium portulacastrum* L.: two halophytes, two strategies to survive in saline habitats. *Plant Physiol. Biochem.* 44, 395–408, <http://dx.doi.org/10.1016/j.jplphys.2006.06.007>.
- Rambaut, A., Drummond, A.J., 2003. Tracer Version 1.2 [Computer Program].
- Rosnow, J.J., Edwards, G.E., Roalson, E.H., 2014. Positive selection of kranz and non-kranz C<sub>4</sub> phosphoenolpyruvate carboxylase amino acids in Suaedoideae (Chenopodiaceae). *J. Exp. Bot.*, <http://dx.doi.org/10.1093/jxb/eru053>.
- Sage, R.F., 2002. Are crassulacean acid metabolism and C<sub>4</sub> photosynthesis incompatible? *Funct. Plant Biol.* 29, 775–785.
- Sage, R.F., Christin, P., Edwards, E.J., 2011. The C<sub>4</sub> plant lineages of planet Earth. *J. Exp. Bot.* 62, 3155–3169.
- Sage, R.F., Koshravesh, R., Sage, T.L., 2014. From proto-kranz to C<sub>4</sub> kranz: building the bridge to C<sub>4</sub> photosynthesis. *J. Exp. Bot.*, <http://dx.doi.org/10.1093/jxb/eru180>.
- Sage, R.F., Kubien, D.S., 2007. The temperature response of C<sub>3</sub> and C<sub>4</sub> photosynthesis. *Plant Cell Environ.* 30, 1086–1106, <http://dx.doi.org/10.1111/j.1365-3040.2007.01682.x>.
- Schäferhoff, B., Müller, K.F., Borsch, T., 2009. Caryophyllales phylogenetics: disentangling Phytolaccaceae and Molluginaceae and description of Microteaceae as a new isolated family. *Willdenowia* 39, 209–228, <http://dx.doi.org/10.3372/wi39.39201>.
- Schütze, P., Freitag, H., Weising, K., 2003. An integrated molecular and morphological study of the subfamily Suaedoideae Ulbr. (Chenopodiaceae). *Plant Syst. Evol.* 239, 257–286, <http://dx.doi.org/10.1007/s00606-003-0013-2>.
- Stamatakis, A., 2006. RAxML-VI-HPC: maximum likelihood-based phylogenetic analyses with thousands of taxa and mixed models. *Bioinformatics* 22, 2688–2690, <http://dx.doi.org/10.1093/bioinformatics/btl446>.
- Stamatakis, A., Hoover, P., Rougemont, J., 2008. A rapid bootstrap algorithm for the RAxML Web Server. *Syst. Biol.* 57, 758–771, <http://dx.doi.org/10.1080/10635150802429642>.
- Taberlet, P., Gielly, L., Pautou, G., Bouvet, J., 1991. Universal primers for amplification of three non-coding regions of chloroplast DNA. *Plant Mol. Biol.* 17, 1105–1109.
- Thiede, J., 2004. Phylogenetics, systematics and classification of the Aizoaceae: a reconsideration based on molecular data. *Schumannia* 4, 51–58.
- Thulin, M., Thiede, J., Liede-Schumann, S., 2012. Phylogeny and taxonomy of *Tribulocarpus* (Aizoaceae): a paraphyletic species and an adaptive shift from zochorous trample burrs to amochorous nuts. *Taxon* 61, 55–66.
- Vaidya, G., Lohmann, D.J., Meier, R., 2011. SequenceMatrix: concatenation software for the fast assembly of multi-gene datasets with character set and codon information. *Cladistics* 27, 171–180, <http://dx.doi.org/10.1111/j.1096-0031.2010.00329.x>.
- Valente, L.M., Britton, A.W., Powell, M.P., Papadopoulos, A.S., Burgoyne, P., Savolainen, V., 2013. Correlates of hyperdiversity in southern African ice plants (Aizoaceae). *Bot. J. Linn. Soc.* 174, 110–129.
- Voznesenskaya, E.V., Koteyeva, N.K., Edwards, G.E., Ocampo, G., 2010. Revealing diversity in structural and biochemical forms of C<sub>4</sub> photosynthesis and a C<sub>3</sub>–C<sub>4</sub> intermediate in genus *Portulaca* L (Portulacaceae). *J. Exp. Bot.* 61, 3647–3662, <http://dx.doi.org/10.1093/jxb/erq178>.
- Wacker, R., 2006. Eine neue und einfache Methode zur polychromatischen Anfärbung von Paraffinschnitten pflanzlicher Gewebe für Durchlicht- und Fluoreszenzmikroskopie. *Mikroskopie* 4, 210–212.
- Wikström, N., Savolainen, V., Chase, M.W., 2001. Evolution of the angiosperms: calibrating the family tree. *Proc. R. Soc. Lond. B* 268, 2211–2220, <http://dx.doi.org/10.1098/rspb.2001.1782>.
- Yu, Y., Harris, A.J., He, X.-J., 2013. RASP (Reconstruct Ancestral State in Phylogenies) 2.1 Beta [Computer Program], Available at <http://mnh.scu.edu.cn/soft/blog/RASP/>